# Mathematical Models of the Alpha-Beta Phase Transition of Quartz

George W. Moss

Dissertation submitted to the Faculty of the
Virginia Polytechnic Institute and State University
in partial fulfillment of the requirements for the degree of

Doctor of Philosophy
in
Mathematics

Robert C. Rogers, Chair
Monte Boisen
Tao Lin
Michael Renardy
Shu Ming Sun

July 27, 1999
Blacksburg, Virginia

Keywords: Phase transition, quartz, incommensurate, bifurcation

# Mathematical Models of the Alpha-Beta Phase Transition of Quartz

George W. Moss

(ABSTRACT)

We examine discrete models with hexagonal symmetry to compare the sequence of transitions with the alpha-inc-beta phase transition of quartz. We examine a model by Parlinski which employs interactions of nearest and next-nearest neighbor atoms. We numerically determine the configurations which lead to minimum energy for a range of parameters. We then use Golubitsky's results on systems with hexagonal symmetry to derive the bifurcation diagram for Parlinski's model. Finally, we study a large class of modifications to Parlinski's model and show that all such modifications have the same bifurcation picture as the original model.

This work received support from the National Science Foundation.

# Acknowledgments

I would first like to thank my advisor, Dr. Robert C. Rogers, for his tremendous support and encouragement over the past few years. I appreciate him leading me to this topic and guiding and teaching me the background necessary for this. It has been a pleasure to work with him.

I also thank the other members of my committee for the guidance they have given and for the time that they have invested in me. The entire department has been a wonderful place to pursue my graduate degree, and I am grateful for all of the professors and fellow students who have helped me along the way.

Finally, I thank my wife, Beverly, for being wonderful to me while I sometimes neglected her. Her love and support has been extremely encouraging at times which were difficult for me. My daughters, Joy and Delie, were a great distraction from math at the end of the day and kept me sane and happy, and I thank them for that.

# Contents

# List of Figures

# List of Tables

# Chapter 1

# Introduction

## 1.1 Phase transition of quartz

Silicon dioxide ($SiO_2$) is one of the most abundant minerals of the earth's crust, and crystalline quartz is the most common of the many phases of $SiO_2$ that exist. At least nine phases of $SiO_2$ have been found to occur, many at high temperature or high pressure. Some of these phases are shown in Figure 1.1 in the temperature and pressure region in which they are favored. A wealth of information on the properties of the different phases of $SiO_2$ can be found in the reference by Sosman [37]. This paper will address only the transition between $\alpha$-quartz and $\beta$-quartz.

The $\alpha$-$\beta$ phase transition of quartz was first discovered by Le Chatelier in 1889 [25] and has generated a great deal of interest and study since then. At temperatures of about 573° C, quartz undergoes a phase change from the higher temperature $\beta$-phase to the lower temperature $\alpha$-phase. This phase transition is accompanied by a change in symmetry, volume, and shape, where the $\beta$-phase has higher symmetry and volume than the $\alpha$-phase.

Quartz can be thought of as $SiO_4$ tetrahedra connected by common oxygen vertices, forming a helix around the c-axis. By focusing on the silicon atoms, it is possible to view the crystal as parallel, interconnected helices as shown in Figure 1.2. There are three evenly-spaced silicon atoms per turn of the helix.

By looking down the vertical axis, it is possible to project the atoms into a two-dimensional hexagonal lattice. These two-dimensional projections of the phases of quartz are shown in Figures 1.3 and 1.4. The lower temperature $\alpha$-phase has a lower symmetry and smaller volume than the higher temperature $\beta$-quartz. Although both phases can be observed on a hexagonal lattice, $\alpha$-quartz has trigonal (3-fold) symmetry while $\beta$-quartz has hexagonal (6-fold) symmetry.

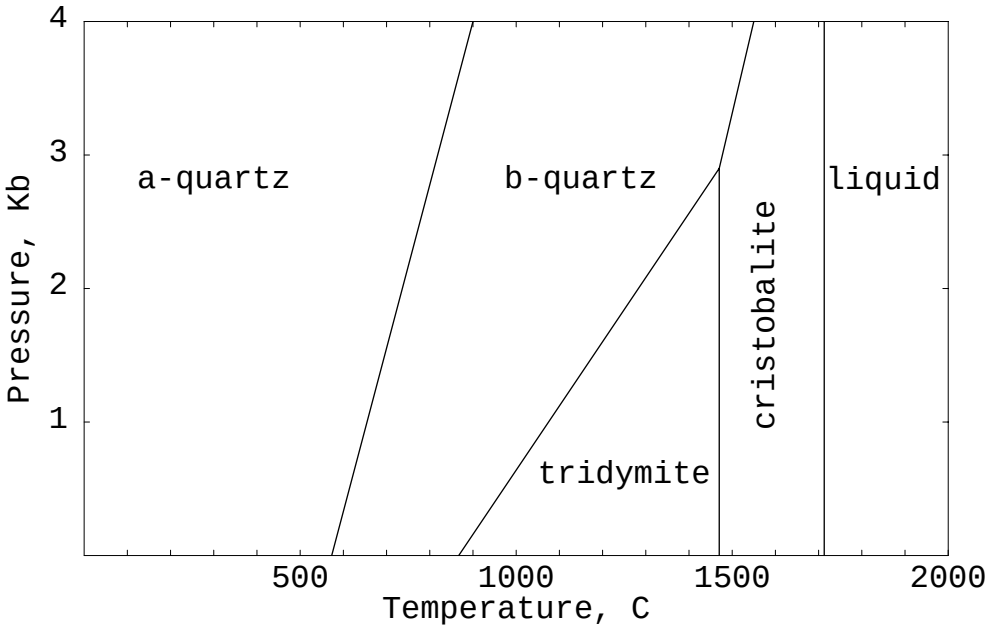


Figure 1.1: The phases of $SiO_2$ in the temperature and pressure regions in which they are favored.

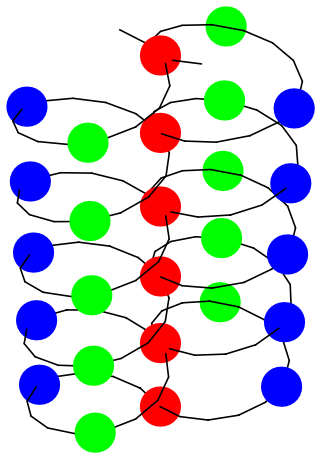

Figure 1.2: Parallel helixes of silicon atoms in a quartz crystal. The axis of the helixes is called the "optic axis." The crystal is assume to be extended periodically.

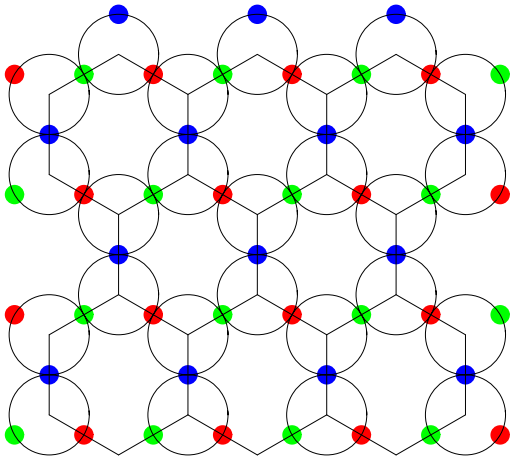

Figure 1.3: Projection of the helixes into a plane perpendicular to the optic axis. High temperature $\beta$ quartz.

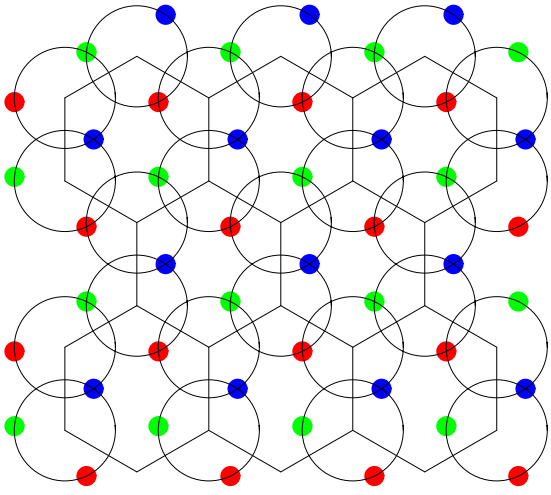

Figure 1.4: Low temperature $\alpha$ quartz. Note the two possible twists that allow atoms to occupy adjacent helixes.

## 1.2 Incommensurate phase

Crystals are solids which are composed of the systematic arrangement of atoms, ions, or molecules, as opposed to amorphous solids which are arranged randomly rather than systematically. Crystals are known for their translational lattice periodicity. Indeed, crystals are traditionally assigned to one of the three-dimensional crystallographic space groups [11, 10]. Recent attention has been given, however, to materials which have perfect three-dimensional long range order but not the translational periodicity seen in crystals. These materials, which fall somewhere in between classical ideal crystals and amorphous systems, are known as incommensurate materials [9]. An extensive list of incommensurate materials with references to major works is given in [35]. In these materials, at least one local property is modulated with a period $q_i$ which is incommensurate to the underlying periodicity $q_p$ of the crystal lattice. In other words,

$$\frac{q_i}{q_p} \neq \frac{M}{N}, \;\; M, N = 1, 2, 3...$$

After almost a certury of research, many scientists were beginning to conclude that all of the important features of the $\alpha$-$\beta$ phase transitions in quartz were known. Then the discovery of an incommensurate phase between the $\alpha$ and $\beta$ phases renewed interest in this phase transition, showing scientists that more accurate experiments could lead to previously unsuspected findings. Incommensurate phases are also found in other crystals related to quartz, e.g. Berlinite ($AlPO_4$), Eucryptite ($LiAlSiO_4$), and Tridymite ($SiO_2$) [17].

In the mid-1970's, both Malov and Sonyushkin [26] and Van Tendeloo *et al.* [41] found evidence of a fine triangular structure between the $\alpha$ and $\beta$ phases of quartz using electron microscopy, producing results similar to those shown in Figure 1.5. In both of these papers, the observance was described as Dauphiné microtwinning. Later, Aslanian and Levanyuk [3] suggested that the triangular structure was due to an incommensurate phase. Experimental work by Bachheimer [5] has confirmed that an intermediate phase does exist for approximately 1.5° C between the $\alpha$ and $\beta$ phases.

The originally observed triangular structure has become known as a $3q$ incommensurate phase because it is composed of the superposition of three modulation waves at 120°, made possible because of the hexagonal symmetry of quartz. The Aslanian and Levanyuk model also suggested that a $1q$ incommensurate phase was possible with only one of the modulation waves.

A stripe incommensurate phase was discovered in quartz under stress using various techniques [1, 6, 18, 36, 42]. Bachheimer [6] found evidence to suggest that the $1q$ phase could exist without stress, and this was confirmed by Bastie *et al.* [7] and Soula *et al.* [38]. With no applied stress, the $1q$ phase is now believed to exist in a temperature region of about 0.05° C between the $\beta$ and $3q$ phases. Thus, the full $\alpha$-$\beta$ transition upon cooling is $\beta \rightarrow 1q\ inc \rightarrow 3q\ inc \rightarrow \alpha$.

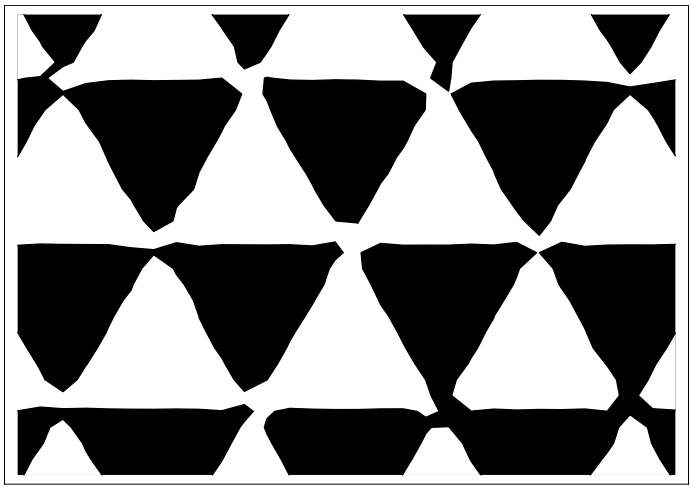

Figure 1.5: Computer-generated simulation of a typical electron micrograph showing the $3q$ phase, similar to those in the literature. Saint Grégoire shows the edge of the triangles to be on the order of 50 nm.

The Aslanian and Levanyuk [3, 4] model which predicted the incommensurate phases was an example of a Landau model. In Landau theory, the free energy is written as

$$F(\eta, T) = \sum_{i=0}^{\infty} F_i(T)\eta^i$$

where $T$ is the temperature and $\eta$ is an order-parameter. The coefficients $F_i$ are determined based on the material under consideration. In quartz, the transition can be modeled with an order-parameter $\eta$ which corresponds to the rotation angle of the $SiO_4$ tetrahedra. For more background on using Landau theory to analyze phase transitions, see [13, 33].

The Aslanian and Levanyuk model (and its relatives) have been studied extensively (see, e.g., [12, 32, 39, 40] and the reviews [15, 23] and the references cited therein). Its most important feature is that under certain conditions, an incommensurate phase has lower energy than either the $\beta$ or $\alpha$-phases in a region close to the transitions point. A third-order term is used to induce a $3q$ pattern such as that illustrated in Figure 1.5, while the fourth-order term favors the $1q$ structure.

Although Landau theory is able to correctly predict much of the behavior of quartz, there are still many open mathematical and physical problems. We hope to address some of these using discrete models.

# Chapter 2

# Bifurcation on a Hexagonal Lattice

In [14], Buzano and Golubitsky studied bifurcation problems with hexagonal symmetry. Their motivation for doing so was to study the planar Bénard problem. In this problem a viscous fluid is contained in a rectangular box with insulated side walls and upper and lower faces which are held at constant temperatures. If the temperature of the lower surface is significantly larger than that of the upper surface, then convection occurs. At the onset of convection in experiments, the fluid usually takes on the form either of rolls or hexagons. The work of Buzano and Golubitsky [14], and later Golubitsky *et al.* [22], while motivated by the Bénard problem, can be applied to any problem involving the hexagonal lattice. Specifically, the rolls and hexagons in the Bénard problem correspond, respectively, to the $1q$ and $3q$ incommensurate phases of quartz. More background into their methods for analyzing bifurcation problems can be found in the earlier works by Sattinger [34] and Golubitsky and Schaeffer [19] and in the volumes [20] and [21]. We present here some of their results and some extensions which will prove to be applicable to our work with quartz. We first present some definitions and notation from [14, 21, 22].

## 2.1 Definitions, notation, and preliminaries

If $\mathbf{w}_1$ and $\mathbf{w}_2$ are any two linearly independent vectors in $\mathbb{R}^2$, then $\{n\mathbf{w}_1 + m\mathbf{w}_2 | n, m \in \mathbb{Z}\}$ is the lattice spanned by $\mathbf{w}_1$ and $\mathbf{w}_2$. We consider a hexagonal lattice, $\Lambda$, spanned by the vectors $\mathbf{w}_1 = (1, 0)$ and $\mathbf{w}_2 = (\cos\frac{\pi}{3}, \sin\frac{\pi}{3}) = (\frac{1}{2}, \frac{\sqrt{3}}{2})$. Since rolls and hexagons are both doubly periodic with repect to a hexagonal lattice, our problems will be posed on a hexagonal lattice.

We define the vector space of all real-valued, smooth, $\Lambda$-periodic functions on $\mathbb{R}^2$ to be $\mathcal{F}^\Lambda$, i.e.

$$\mathcal{F}^\Lambda = \{f(\mathbf{X}) \in C^1(\mathbb{R}^2) \mid f(\mathbf{X} + n\mathbf{w}_1 + m\mathbf{w}_2) = f(\mathbf{X}) \; \forall n, m \in \mathbb{Z}\}.$$

Using a double Fourier series, any function in $\mathcal{F}^\Lambda$ can be written as

$$f(\mathbf{X}) = \sum_{\mathbf{j}\in\mathbb{Z}^2} C_{\mathbf{j}} e^{i(j_1\mathbf{k}_1+j_2\mathbf{k}_2)\cdot\mathbf{X}}$$

Here $C_j = \bar{C}_{-j}$ and $\mathbf{k}_1$ and $\mathbf{k}_2$ are basis vectors for the reciprocal lattice of $\Lambda$. The reciprocal lattice vectors are chosen so that $\mathbf{k}_i \cdot \mathbf{w}_j = 2\pi\delta_{ij}$ where $\delta_{ij}$ is the Kronecker delta function. This means that $\mathbf{k}_1 = \frac{4\pi}{\sqrt{3}}(\frac{\sqrt{3}}{2}, -\frac{1}{2})$ and $\mathbf{k}_2 = \frac{4\pi}{\sqrt{3}}(0, 1)$. For ease of notation, we define the vectors $\mathbf{k}_3 = -\mathbf{k}_1 - \mathbf{k}_2$ and $\mathbf{k}_{j+3} = -\mathbf{k}_j$ for $j = 1, 2, 3$.

It should be noted that in [14], the $\mathbf{k}$-vectors were chosen so that $\mathbf{k}_1 - \mathbf{k}_2 + \mathbf{k}_3 = 0$, but they were chosen so that $\mathbf{k}_1 + \mathbf{k}_2 + \mathbf{k}_3 = 0$ in [22]. We use the notation of [22].

The set of Euclidean motions includes all rigid motions of the plane, i.e., translations, rotations, and reflections.If $\sigma$ is a Euclidean motion of $\mathbb{R}^2$ and $f : \mathbb{R}^2 \to \mathbb{R}$ is a function, then $\sigma$ acts on $f$ by $T_\sigma f(\mathbf{X}) = f(\sigma(\mathbf{X}))$. Let $G_n$ denote the subgroup of Euclidean motions which leaves $\mathcal{F}^\Lambda$ invariant, i.e. $\gamma \in G_n$ if $T_\gamma(\mathcal{F}^\Lambda) = \mathcal{F}^\Lambda$. This symmetry group is given by the semidirect sum $G_n = D_6 \dot{+} T^2$ [14].

Let $N$ denote the smallest subspace of $\mathcal{F}^\Lambda$ having the same symmetry group. Then $N$ is defined by

$$N = \{f(\mathbf{X}) = \sum_{j=1}^{6} z_j e^{i\mathbf{k}_j\cdot\mathbf{X}},\ z_j \in \mathbb{C},\ z_{j+3} = \bar{z}_j \text{ for } j = 1, 2, 3\}.$$

Since $z_{j+3} = \bar{z}_j$, we can represent any $f \in N$ by the triple $(z_1, z_2, z_3)$. This means that we can identify $N$ with $\mathbb{C}^3$. We now describe the action of $G_n$ on $N$ (or $\mathbb{C}^3$).

The symmetry group $\mathrm{D}_3$ is generated by rotation of 120° and reflection in a vertical plane. These elements are shown as

$$\begin{aligned} r &: (z_1, z_2, z_3) \mapsto (z_2, z_3, z_1) \\ \sigma_v &: (z_1, z_2, z_3) \mapsto (z_1, z_3, z_2). \end{aligned}$$

The group $\mathrm{D}_6$ includes the elements of $\mathrm{D}_3$ together with the complex conjugation mapping $c : \mathbf{z} \mapsto \bar{\mathbf{z}}$.

This means that the eleven nontrivial elements of $\mathrm{D}_6$ act on N (or $\mathbb{C}^3$) by sending $(z_1, z_2, z_3)$ to

$$\begin{array}{llll} (a) & (\bar{z}_3, \bar{z}_1, \bar{z}_2) & (b) & (z_2, z_3, z_1) \\ (c) & (\bar{z}_1, \bar{z}_2, \bar{z}_3) & (d) & (z_3, z_1, z_2) \\ (e) & (\bar{z}_2, \bar{z}_3, \bar{z}_1) & (f) & (z_2, z_1, z_3) \\ (g) & (\bar{z}_3, \bar{z}_2, \bar{z}_1) & (h) & (z_1, z_3, z_2) \\ (i) & (\bar{z}_2, \bar{z}_1, \bar{z}_3) & (j) & (z_3, z_2, z_1) \\ (k) & (\bar{z}_1, \bar{z}_3, \bar{z}_2) & & \end{array} \tag{2.1}$$

The translations $\mathbf{X} \mapsto \mathbf{X} + \mathbf{d}$ are described by the action $T^2 \times \mathbb{C}^3 \to \mathbb{C}^3$:

$$(s,t) \cdot \mathbf{z} = (e^{is} z_1, e^{-i(s+t)} z_2, e^{it} z_3) \tag{2.2}$$

where $s = \mathbf{k}_1 \cdot \mathbf{d}$ and $t = \mathbf{k}_3 \cdot \mathbf{d}$.

It is possible in some problems to have a horizontal mid-plane symmetry in addition to the hexagonal symmetry in the plane. With this additional symmetry, the subgroup that leaves $\mathcal{F}^\Lambda$ invariant is $G_s = G_n \oplus Z_2$ [22]. The subscripts on $G_n$ and $G_s$ stand for nonsymmetric and symmetric, respectively.

We use the notation $u_i = z_i \bar{z}_i$ and define the three elementary symmetric polynomials $\sigma_j$ as

$$\sigma_1 = u_1 + u_2 + u_3, \;\; \sigma_2 = u_1 u_2 + u_1 u_3 + u_2 u_3, \;\; \sigma_3 = u_1 u_2 u_3.$$

Also let $q = z_1 z_2 z_3 + \bar{z}_1 \bar{z}_2 \bar{z}_3$. Buzano and Golubitsky [14] prove the following theorems about these variables.

**Theorem 2.1.** *All real-valued functions of $\sigma_1$, $\sigma_2$, $\sigma_3$, and $q$ are invariant under $G_n$ (and $G_s$). Further, all smooth functions which are invariant under $G_n$ (or $G_s$) must be functions of those four variables only.*

**Theorem 2.2.** *If $g : \mathbb{C}^3 \times \mathbb{R} \to \mathbb{C}^3$ commutes with the group $G_n$, then $g$ has the form*

$$g(z_1, z_2, z_3, \lambda) = (H_1 z_1 + P_1 \bar{z}_2 \bar{z}_3, \;\; H_2 z_2 + P_2 \bar{z}_1 \bar{z}_3, \;\; H_3 z_3 + P_3 \bar{z}_1 \bar{z}_2) \tag{2.3}$$

*where $H_j = h_1 + u_j h_3 + u_j^2 h_5$ and $P_j = p_2 + u_j p_4 + u_j^2 p_6$ and where $h_i$ and $p_i$ are invariant functions of $\sigma_1$, $\sigma_2$, $\sigma_3$, $q$, and $\lambda$.*

*In the symmetric case ($g$ commutes with $G_s$), only odd powers of $\mathbf{z}$ are allowed in the amplitude equations because of the additional symmetry. This means that $g$ is further restricted to the form*

$$g(z_1, z_2, z_3, \lambda) = (L_1 z_1 + q M_1 \bar{z}_2 \bar{z}_3, \;\; L_2 z_2 + q M_2 \bar{z}_1 \bar{z}_3, \;\; L_3 z_3 + q M_3 \bar{z}_1 \bar{z}_2) \tag{2.4}$$

*where $L_j = l_1 + u_j l_3 + u_j^2 l_5$ and $M_j = m_5 + u_j m_7 + u_j^2 m_9$ and where $l_i$ and $m_i$ are functions of $\sigma_1$, $\sigma_2$, $\sigma_3$, $q^2$, and $\lambda$.*

In our bifurcation problems, we look for solutions to $g(\mathbf{z}, \lambda) = 0$ where $g : \mathbb{C}^3 \times \mathbb{R} \to \mathbb{C}^3$ commutes with the group $G$ (either $G_n$ or $G_s$). Since $g(\gamma \mathbf{z}, \lambda) = \gamma g(\mathbf{z}, \lambda)$, if $\mathbf{z}$ is a solution to $g(\mathbf{z}, \lambda) = 0$, then so is the entire orbit of $\mathbf{z}$, defined by

$$G\mathbf{z} = \{\gamma \mathbf{z} \mid \gamma \in G\}.$$

We can classify the symmetry of a solution $\mathbf{z}$ by the isotropy subgroup $\Sigma_{\mathbf{z}}$, the subgroup of $G$ which leaves $\mathbf{z}$ invariant,

$$\Sigma_{\mathbf{z}} = \{\gamma \in G \mid \gamma \mathbf{z} = \mathbf{z}\}.$$

We now use the fact that if $\mathbf{w}$ and $\mathbf{z}$ lie on the same orbit of $G_n$ (or $G_s$), then their isotropy subgroups are conjugate. This allows us to find all solutions by finding the isotropy subgroups of specific representatives on each orbit. In the next section we show some of the results of [14] in the characterization of all solutions of $g(\mathbf{z}, \lambda) = 0$ for the nonsymmetric case. Section 2.3 covers similar results for the symmetric case presented in [22], and Section 2.4 extends some of the results from the nonsymmetric case.

## 2.2 The nonsymmetric case

In the following theorem, Buzano and Golubitsky [14] calculate the isotropy subgroups for each orbit and give physically suggestive names to each of the orbit types. We are using the notation $z_j = x_j + iy_j$, $j = 1, 2, 3$ and $\mathbf{z} = (z_1, z_2, z_3)$.

**Theorem 2.3.** *For each orbit of the action of $G_n$ on $\mathbb{C}^3 = \{(z_1, z_2, z_3)\}$, a unique representative is given in Table 2.1 along with the (conjugacy class of) isotropy subgroup associated with that orbit. In the last column we give the equation to which the system $g(\mathbf{z}, \lambda) = 0$ reduces at the representative point on the orbit.*

*Remark.* In the original proof in [14], the Buzano and Golubitsky show that each orbit must pass through the half-plane defined by $y_1 = y_3 = 0$ and $y_2 > 0$. The proof below follows that proof, but we use the table from [22] in which the isotropy subgroups are more consistent. This requires that we use an element (or elements) from $G_n$ to transform the orbit representative given in the original proof to the one given in Table 2.1.

*Proof.* Let $\mathbf{z}$ be in $\mathbb{C}^3$. Our first goal is to use group elements to "move" $\mathbf{z}$ to the half-plane defined by $y_1 = y_3 = 0$ and $y_2 > 0$. To do this we first want to choose some $(s, t) \in T^2$ so that $(s, t) \cdot \mathbf{z} = (x_1, x_2 + iy_2, x_3)$. To find the appropriate $(s, t)$, write $z_1 = r_1 e^{i\theta}$ where $r_1 \geq 0$ is real and $\theta \in [0, 2\pi)$. Then $e^{is} z_1 = r_1 e^{i(s+\theta)}$. If $s = 2\pi - \theta$, then $e^{is} z_1 = r_1$, so $e^{is} z_1$ is real and positive. We can choose $t$ similarly so that $e^{it} z_3 = r_3$ which is both real and positive.

By applying the group element

$$c : (z_1, z_2, z_3) \mapsto (\bar{z}_1, \bar{z}_2, \bar{z}_3)$$

if necessary, we ensure that $y_2 \geq 0$. Now $\mathbf{z} = (x_1, x_2 + iy_2, x_3)$ with $x_1$, $x_3$, and $y_2$ nonnegative.

It is easy to see that the number of $u_i$'s that are equal to each other is invariant under $G_n$. For this reason, we can choose representatives of the orbits by considering the cases where different numbers of the $u_i$'s are equal.

First, assume that $u_1 = u_2 = u_3 = u$. If $u = 0$, then we are in the trivial case, where the isotropy subgroup is $G_n$. If $u \neq 0$, then $u$ can either be real or complex.

Table 2.1: Categories of solutions, orbit representatives, and isotropy subgroups for the nonsymmetric case.

| | nomenclature | orbit representative | isotropy subgroup | equations |
|---|---|---|---|---|
| I | Trivial solution | $\mathbf{z} = 0$ | $G_n$ | |
| II | Rolls | $x_1 > 0,\ x_2 = x_3 = 0$<br>$y_1 = y_2 = y_3 = 0$ | $\mathrm{S}^1 + \{\sigma_v, c\}$ | $H_1 = 0$ |
| III | Hexagons | $x_1 = x_2 = x_3 \neq 0$<br>$y_1 = y_2 = y_3 = 0$ | $\mathrm{D}_3 + \{c\}$ | $H_1 + x_1 P_1 = 0$ |
| IV | Rectangles | $x_1 \neq x_2 = x_3 \neq 0$<br>$y_1 = y_2 = y_3 = 0$ | $Z_2^2 = \{\sigma_v, c\}$ | $H_2 + x_1 P_2 = 0$<br>$x_1[h_3 + (x_1^2 + x_2^2)h_5$<br>$+x_1 x_2^2 p_6] = p_2$ |
| V | Triangles | $x_1 = x_2 = x_3$<br>$y_1 = y_2 = y_3 \neq 0$ | $\mathrm{D}_3$ | $H_1 = 0$<br>$P_1 = 0$ |
| VI | | $x_2 = x_3 > 0$<br>$u_1 \neq u_2$<br>$y_1 > 0,\ y_2 = y_3 = 0$ | $Z_2 = \{\sigma_v\}$ | $H_2 = P_2 = 0$<br>$h_3 + (u_1 + u_2)h_5 = 0$<br>$p_4 + (u_1 + u_2)p_6 = 0$ |
| VII | | $y_1 = y_2 = y_3 = 0$<br>$u_2 < u_1 < u_3$ | $Z_2 = \{c\}$ | $x_1 H_1 + x_2 x_3 P_1 = 0$<br>$x_2 H_2 + x_1 x_3 P_2 = 0$<br>$x_3 H_3 + x_1 x_2 P_3 = 0$ |
| VIII | | $y_1 = y_3 = 0,\ y_2 > 0$<br>$u_2 < u_1 < u_3$ | $\{1\}$ | $h_1 = h_3 = h_5 = 0$<br>$p_2 = p_4 = p_6 = 0$ |

where $\mathrm{S}^1$: $\mathbf{z} \mapsto (z_1, e^{-it} z_2, e^{it} z_3)$
$\mathrm{D}_3$: permutation group of $z_1, z_2, z_3$
$\sigma_v$: $\mathbf{z} \mapsto (z_1, z_3, z_2)$
$c$: $\mathbf{z} \mapsto \bar{\mathbf{z}}$

If $u$ is real ($y_2 = 0$), then $\mathbf{z} = (x, \pm x, x)$. By $(\pi, \pi) \in T^2$, we get that

$$(x, -x, x) \mapsto (-x, -x, -x) = -(x, x, x)$$

so that there are two orbits, $\pm(x, x, x)$, which represent the two types of hexagons. Each of these has isotropy subgroup $\mathrm{D}_6$.

If $u$ is not real ($y_2 > 0$), then $x_1 = x_3 = |z_2|$ which represents triangles. This means that $z_2 = x_1 e^{i\theta}$ for some $\theta$. An alternative representative orbit is given by $z_1 = z_2 = z_3 = x_1 e^{i\frac{\theta}{3}}$. This can be seen by choosing $(\frac{\theta}{3}, \frac{\theta}{3}) \in T^2$ so that

$$(\tfrac{\theta}{3}, \tfrac{\theta}{3}) \cdot (x_1, x_1 e^{i\theta}, x_1) = (x_1 e^{i\frac{\theta}{3}}, x_1 e^{i\frac{\theta}{3}}, x_1 e^{i\frac{\theta}{3}}).$$

From this alternate representation, it is easy to see that the isotropy subgroup is $\mathrm{D}_3$.

Next, consider the case that two of the $u_i$'s are equal and the third is different. We can permute the $u_i$'s using elements of $G_n$, so we can choose which two we want to be equal. If the identical two are equal to zero, say $u_2 = u_3 = 0$, then we are in an orbit of rolls. Here the isotropy subgroup is $\mathrm{D}_6$.

If the two identical $u_i$'s are not zero, say $u_1 = u_3 \neq 0$, then there are two cases - either $z_2$ is real or not. If $z_2$ is real, then the orbits are of the rectangle type and the isotropy subgroup is $\{\sigma_v, c\}$. If $z_2$ is not real, then we have $x_1 = x_3 > 0$, $y_2 > 0$, and $u_1 \neq u_2$. This is case VI, where the isotropy subgroup is $\{\sigma_v\}$.

Finally, we must consider the case that all of the $u_i$'s are distinct. By permutation, we may assume that $u_2 < u_1 < u_3$. We have to consider whether $z_2$ is real or not. If $z_2$ is real ($y_2 = 0$), then $x_2^2 < x_1^2 < x_3^2$. This is case VII, and the isotropy subgroup is $\{c\}$. If $z_2$ is not real ($y_2 > 0$), then we are in case VIII where the isotropy subgroup has no nontrivial elements.

Now we turn our attention to deriving the reduced equations given for each case. This will enable us to determine whether or not $g(\mathbf{z}, \lambda) = 0$ has a solution of a given orbit type.

**(II)** For type II, we have $\mathbf{z} = (x_1, 0, 0)$ so that $g(\mathbf{z}, \lambda) = (H_1 x_1, 0, 0)$. This means that the reduced equation will be $H_1 = 0$ since $x_1$ is assumed to be positive.

**(III)** For type III, we have the representative $\mathbf{z} = (x_1, x_1, x_1)$. Then $g(\mathbf{z}, \lambda) = (H_1 x_1 + P_1 x_1^2, H_1 x_1 + P_1 x_1^2, H_1 x_1 + P_1 x_1^2)$, so the determining equation is simply $H_1 + P_1 x_1 = 0$.

**(IV)** For solutions of type IV, we have $x_2 = x_3 > 0$, so we can reduce (2.3) to $x_1 H_1 + x_2^2 P_1 = 0$ and $H_2 + x_1 P_2 = 0$. Multiplying the second by $x_1$ and subtracting the first and then dividing the result by $u_1 - u_2$ (which is nonzero), gives

$$x_1[h_3 + h_5(x_1^2 + x_2^2) + x_1 x_2^2 p_6] = p_2.$$

This is the given result.

**(V)** For solutions of type V, we have $u_1 = u_2 = u_3$. This means that $H_1 = H_2 = H_3$ and $P_1 = P_2 = P_3$, so we just have $z_1 H_1 + \bar{z}_1 \bar{z}_1 P_1 = 0$. We can write this as two equations with reals coordinates as

$$\begin{aligned} x_1 H_1 + (x_1^2 - y_1^2) P_1 = 0, \text{and} \\ y_1 H_1 - 2 x_1 y_1 P_1 = 0. \end{aligned}$$

If $x_1 = 0$, then clearly $H_1 = 0$ and $P_1 = 0$. If $x_1 \neq 0$ then multiply the first equation by $y_1$ and the second equation by $x_1$ and subtract the result. This reduces to $y_1(x_1^2 + y_1^2)P_1 = 0$. It is assumed that $y_1 \neq 0$, so it must be true that $P_1 = 0$. Using this in the second equation implies that $H_1 = 0$ also.

**(VI)** Solutions on orbits of type VI have $u_1 \neq u_2 = u_3$ with $y_2 = y_3 = 0$. This allows us to reduce (2.3) to

$$\begin{aligned} (x_1 + i y_1) H_1 + x_2^2 P_1 = 0, \text{and} \\ x_2 H_2 + x_2 (x_1 - i y_1) P_2 = 0. \end{aligned}$$

Using the fact that $H_j$ and $P_j$ are real, we can focus on the imaginary part of each of these equations. These are $y_1 H_1 = 0$ and $y_1 P_2 = 0$. Now it is assumed that $y_1 \neq 0$, so this gives $H_1 = P_2 = 0$. Using this in the original equations leads to the fact that $P_1 = H_2 = 0$ also. An equivalent way to write these four equations is $H_2 = P_2 = H_1 - H_2 = P_1 - P_2 = 0$. Now

$$H_1 - H_2 = h_3(u_1 - u_2) + h_5(u_1^2 - u_2^2),$$

so dividing by $u_1 - u_2$ (which is nonzero) gives $h_3 + h_5(u_1 + u_2) = 0$. Dividing $P_1 - P_2 = 0$ by $u_1 - u_2$ produces $p_4 + p_6(u_1 + u_2) = 0$ in a similar manner.

**(VII)** Now for VII, we have $y_1 = y_2 = y_3 = 0$, so (2.3) becomes

$$\begin{aligned} x_1 H_1 + x_2 x_3 P_1 = 0 \\ x_2 H_2 + x_1 x_3 P_2 = 0 \\ x_3 H_3 + x_1 x_2 P_3 = 0. \end{aligned}$$

These are the desired equations for type VII.

**(VIII)** For orbits of type VIII, we observe that (2.3) has a linear structure which can be written in matrix form as:

$$\left[\begin{array}{ccc|ccc} x_1 & & & x_2 x_3 & & \\ & x_2 & & & x_1 x_3 & \\ & & x_3 & & & x_1 x_2 \\ \hline 0 & & & x_3 y_2 & & \\ & y_2 & & & 0 & \\ & & 0 & & & x_1 y_2 \end{array}\right] \left[\begin{array}{c} H_1 \\ H_2 \\ H_3 \\ P_1 \\ P_2 \\ P_3 \end{array}\right] = 0. \tag{2.5}$$

Here, we are using the real coordinates and assuming that $y_1 = y_3 = 0$. The determinant of the matrix is found to be $(x_1y_2x_3)^3$, and since $y_2 \neq 0$, the matrix is invertible so that (2.3) reduces to

$$H_j = 0, \;\; P_j = 0, \;\; j = 1, 2, 3. \tag{2.6}$$

It is easy to see that (2.6) has the matrix form

$$\left[\begin{array}{c|c} V & 0 \\ \hline 0 & V \end{array}\right] \begin{bmatrix} h_1 \\ h_3 \\ h_5 \\ p_2 \\ p_4 \\ p_6 \end{bmatrix} = 0 \tag{2.7}$$

where $V$ is the Vandermonian matrix

$$\begin{bmatrix} 1 & u_1 & u_1^2 \\ 1 & u_2 & u_2^2 \\ 1 & u_3 & u_3^2 \end{bmatrix}$$

and $\det(V) = (u_1 - u_2)(u_1 - u_3)(u_2 - u_3)$. Thus for solutions of type VIII, $\det(V) \neq 0$, so the determining equations for type VIII are

$$h_1 = h_3 = h_5 = p_2 = p_4 = p_6 = 0.$$

□

The preceding theorem gives us a method of calculating solutions to a problem with hexagonal symmetry. Buzano and Golubitsky [14] also made progress into determining the stability of these solutions by simplifying the calculation of eigenvalues of the Jacobian of $g$.

They write the problem in real coordinates as

$$g(\mathbf{x}, \mathbf{y}, \lambda) = \begin{pmatrix} g_1 \\ g_2 \\ g_3 \\ g_4 \\ g_5 \\ g_6 \end{pmatrix} = \begin{pmatrix} H_1x_1 + P_1(x_2x_3 - y_2y_3) \\ H_2x_2 + P_2(x_1x_3 - y_1y_3) \\ H_3x_3 + P_3(x_1x_2 - y_1y_2) \\ H_1y_1 + P_1(-x_2y_3 - y_2x_3) \\ H_2y_2 + P_2(-x_1y_3 - y_1x_3) \\ H_3y_3 + P_3(-x_1y_2 - y_1x_2) \end{pmatrix}. \tag{2.8}$$

**Theorem 2.4.** *Suppose that $g(\mathbf{x}, \mathbf{y}, \lambda) = 0$. Then the eigenvalues of $dg_{(\mathbf{x},\mathbf{y})}$ for the different types of solutions are as follows. The multiplicity is given in parentheses following the eigenvalue.*

**(I)** *$h_1(0, 0, \lambda)$ (6);*

**(II)** *$A$, $D-E$ (2), $D+E$ (2), 0 where $A = x_1\frac{\partial H_1}{\partial x_1}$, $D = -u_1h_3 - u_1^2h_5$, and $E = x_1p_2$;*

**(III)** *$A-B$ (2), $A+2B$, $3\alpha$, 0 (2) where $A = \frac{\partial g_1}{\partial x_1}$, $B = \frac{\partial g_1}{\partial x_2}$, and $\alpha = -x_1P_1$;*

**(IV)** *$D-E$, $\alpha+2\delta$, 0 (2),*

*and the remaining two eigenvalues for solutions of type IV are the eigenvalues of the $2\times 2$ matrix*

$$\begin{bmatrix} A & 2B \\ C & D+E \end{bmatrix}$$

*where $A = \frac{\partial g_1}{\partial x_1}$, $B = \frac{\partial g_1}{\partial x_2}$, $C = \frac{\partial g_2}{\partial x_1}$, $D = \frac{\partial g_2}{\partial x_2}$, $E = \frac{\partial g_2}{\partial x_3}$, $\alpha = H_1$, and $\delta = -x_1P_2$.*

*Remark.* The authors were unable to substantially simplify the calculation of the eigenvalues for the other cases, but this is inconsequential for our application of the results.

*Proof.* We will show here the proof only for case IV. This is the only case where my deviation from the notation of [14] in preference of [22] changes the proof and results of this theorem. Even though the notation is slightly different, this proof still follows the form of the proof in [14].

Suppose that $\gamma$ is an element of the group $G_n$. Then $g(\gamma\cdot\mathbf{z},\lambda) = \gamma\cdot g(\mathbf{z},\lambda)$. Then differentiating using the chain rule gives that

$$dg_{\gamma\cdot\mathbf{z}}(\gamma\cdot\mathbf{z})\cdot\gamma = \gamma\cdot dg_{\mathbf{z}}(\mathbf{z}).$$

Now if $\gamma\in\Sigma_{\mathbf{z}}$, then $\gamma\cdot\mathbf{z}=\mathbf{z}$, so that

$$dg_{\mathbf{z}}\cdot\gamma = \gamma\cdot dg_{\mathbf{z}}.$$

This means that $dg$ commutes with elements of the isotropy subgroup of $\mathbf{z}$.

The isotropy subgroup for solutions of type IV are given by $\{\sigma_v, c\}$, where $\sigma_v : \mathbf{z}\mapsto(z_1,z_3,z_2)$ and $c$ is the complex conjugation. The matrix which corresponds to $c$ in real coordinates is given by

$$Q_3 = \begin{bmatrix} I_3 & 0 \\ 0 & -I_3 \end{bmatrix} \tag{2.9}$$

Since $dg_{\mathbf{z}}Q_3 = Q_3dg_{\mathbf{z}}$, then $dg_{\mathbf{z}}$ must have the form

$$dg_{\mathbf{z}} = \begin{bmatrix} R & 0 \\ 0 & S \end{bmatrix}. \tag{2.10}$$

Now $\sigma_v$ has the corresponding matrix form

$$Q_7 = \begin{bmatrix} J & 0 \\ 0 & J \end{bmatrix}, \tag{2.11}$$

where

$$J = \begin{bmatrix} 1 & 0 & 0 \\ 0 & 0 & 1 \\ 0 & 1 & 0 \end{bmatrix}. \tag{2.12}$$

Since $dg_{\mathbf{z}}$ must also commute with $Q_7$, this means that $dg_{\mathbf{z}}$ must have the form

$$dg_{\mathbf{z}} = \left[\begin{array}{ccc|ccc} A & B & B & & & \\ C & D & E & & 0 & \\ C & E & D & & & \\ \hline & & & \alpha & \beta & \beta \\ & 0 & & \gamma & \delta & \epsilon \\ & & & \gamma & \epsilon & \delta \end{array}\right]. \tag{2.13}$$

Now suppose that $\gamma_t$ is a differentiable curve in $G_n$ where $\gamma_0$ is the identity and assume that $g(\mathbf{z}, \lambda) = 0$. Since $g$ vanishes on orbits of the action of $G_n$, then we have $g(\gamma_t \cdot \mathbf{z}, \lambda) = 0$. Differentiating this with respect to $t$ and evaluating at $t = 0$ yields $dg_{\mathbf{z}} v = 0$ where $v = d(\gamma_t \cdot \mathbf{z})/dt|_{t=0}$. If $\gamma_t$ is a curve in $G_n$ that crosses $\Sigma_{\mathbf{z}}$ with nonzero speed, then $v \neq 0$ and $dg_{\mathbf{z}}$ has $v$ as an eigenvector corresponding to the zero eigenvector.

Consider the curve of group elements $t \mapsto (e^{it} z_1, e^{it} z_2, z_3)$. If we differentiate with respect to $t$ and evaluate at $t = 0$, then we obtain $(iz_1, iz_2, 0)$. Evaluating this at $\mathbf{z} = (x_1, x_2, x_2)$ (the orbit representative for type IV), then we get in real coordinates

$$v_1 = (0, 0, 0, x_1, x_2, 0).$$

Doing the same thing with the curve $t \mapsto (e^{it} z_1, z_2, e^{it} z_3)$ yields the eigenvector

$$v_2 = (0, 0, 0, x_1, 0, x_2).$$

Since both $v_1$ and $v_2$ are in the kernel of $dg_{\mathbf{z}}$, then the lower right-hand $3 \times 3$ matrix in 2.13 has only one nonzero eigenvalue. This is the eigenvalue given by its trace $\alpha + 2\delta$. Notice that for type IV, $\alpha = \frac{\partial g_4}{\partial y_1} = H_1$ and $\delta = \frac{\partial g_5}{\partial y_2} = H_2 = -x_1 P_2$.

The eigenvalues associated with the upper left-hand $3 \times 3$ matrix in 2.13 are harder to find. It is easy to see that $(0, 1, -1)$ is an eigenvector of

$$\begin{bmatrix} A & B & B \\ C & D & E \\ C & E & D \end{bmatrix} \tag{2.14}$$

associated with the eigenvalue $D-E$. Also, the vectors $(1,0,0)$ and $(0,1,1)$ span an invariant supspace of the $3 \times 3$ matrix. The matrix restricted to this subspace is given by the $2 \times 2$ matrix

$$\begin{bmatrix} A & 2B \\ C & D+E \end{bmatrix}. \tag{2.15}$$

Thus the remaining two eigenvalues of $dg_{\mathbf{z}}$ are the eigenvalues of this $2 \times 2$ matrix. □

## 2.3 The symmetric case

The planar Bénard problem shows vastly different results depending on the boundary conditions of its faces. If the boundary conditions on the upper and lower faces are the same, then the problem has a reflectional symmetry in the horizontal midplane. In other words, $-g(\mathbf{z},\lambda) = g(-\mathbf{z},\lambda)$. The above material from Buzano and Golubitsky [14] did not assume this additional symmetry, but the paper by Golubitsky *et al.* [22] does address this.

**Theorem 2.5.** *For each orbit of the action of $G_s$ on $\mathbb{C}^3 = \{(z_1,z_2,z_3)\}$, a unique representative is given in Table 2.2 along with the isotropy subgroup associated with that orbit.*

Golubitsky *et al.* were also successful in determining the stability of the various branches of solutions, as shown in the following theorem.

**Theorem 2.6.** *Assume that $\dot{\mathbf{z}} = g(\mathbf{z},\lambda)$ is of the form (2.4) with*

$$\begin{aligned} l_1(0) = 0,\ l_{1,\lambda}(0) = 0,\ l_{1,\sigma_1}(0) + l_3(0) \neq 0,\ 2l_{1,\sigma_1}(0) + l_3(0) \neq 0, \\ 3l_{1,\sigma_1}(0) + l_3(0) \neq 0,\ l_3(0) \neq 0,\ m_5(0) \neq 0. \end{aligned} \tag{2.16}$$

*Then there are precisely four non-trivial branches of solutions to $g(\mathbf{z},\lambda) = 0$ in the neighborhood of $(\mathbf{z},\lambda) = 0$ corresponding one each to rolls, hexagons, regular triangles, and the patcwork quilt. These branches are supercritical if:*

- *Rolls:* $(l_{1,\sigma_1}(0) + l_3(0))l_{1,\lambda} < 0$,
- *Hexagons and Regular triangles:* $(3l_{1,\sigma_1}(0) + l_3(0))l_{1,\lambda} < 0$,
- *Patchwork quilt:* $(2l_{1,\sigma_1}(0) + l_3(0))l_{1,\lambda} < 0$.

*If any of these inequalities are reversed, the corresponding branch is subcritical.*

Table 2.2: Categories of solutions, orbit representatives, and isotropy subgroups for the symmetric case.

| | nomenclature | orbit representative | isotropy subgroup |
|---|---|---|---|
| I | Trivial solution | $\mathbf{z} = 0$ | $G_s$ |
| II | Rolls | $x_1 > 0,\ y_1 = z_2 = z_3 = 0$ | $\mathrm{S}^1 + \{\sigma_v, c, F_3\}$ |
| III | Hexagons | $x_1 = x_2 = x_3 > 0$ | $\mathrm{D}_3 + \{c\}$ |
| | | $y_1 = y_2 = y_3 = 0$ | |
| IV | Patchwork quilt | $x_2 = x_3 > 0$ | $\{\sigma_v, c, F_1\}$ |
| | | $z_1 = y_2 = y_3 = 0$ | |
| V | Regular triangles | $x_1 = x_2 = x_3 = 0$ | $\mathrm{D}_3 + \{\bar{\sigma_h}\}$ |
| | | $y_1 = y_2 = y_3 > 0$ | |
| VI | Triangles | $x_1 = x_2 = x_3 > 0$ | $\mathrm{D}_3$ |
| | | $y_1 = y_2 = y_3 \neq 0$ | |
| VII | Rectangles | $0 \neq x_1 \neq x_2 = x_3 > 0$ | $Z_2^2 = \{\sigma_v, c\}$ |
| | | $y_1 = y_2 = y_3 \neq 0$ | |
| VIII | Imaginary rectagles | $x_1 = x_2 = x_3 = 0$ | $Z_2^2 = \{\sigma_v, \bar{\sigma_h}\}$ |
| | | $0 \neq y_1 \neq y_2 = y_3 > 0$ | |
| IX | Bimodal | $x_1 > x_2 > x_3 = 0$ | $Z_2 = \{F_3, c\}$ |
| | | $y_1 = y_2 = y_3 = 0$ | |

where $\mathrm{S}^1$, $\mathrm{D}_3$,$\sigma_v$, and $c$ are given in Table 2.1 and
$\bar{\sigma_h}$: $\mathbf{z} \mapsto -\bar{\mathbf{z}}$
$\mathrm{F}_1$: $\mathbf{z} \mapsto (-z_1, z_2, z_3)$
$\mathrm{F}_3$: $\mathbf{z} \mapsto (z_1, z_2, -z_3)$

## 2.4 Extension of the results

In [22], Golubitsky *et al.* were able to successfully classify the number and nature of the steady state solution of $g(\mathbf{z}, \lambda) = 0$ for the symmetric problem. However, because of the more complicated nature of the nonsymmetric problem, Buzano and Golubitsky [14] merely classified the solutions for three specific examples which showed many interesting properites. The examples that they considered were

$$\begin{array}{llllll}
(1) & h_1 = -\lambda, & h_3 = 1, \quad h_5 = 0, & p_2 = 1, & p_4 = 0, & p_6 = 0, \\
(2) & h_1 = -\lambda + \sigma_1^2, & h_3 = a, \quad h_5 = 0, & p_2 = 1, & p_4 = 0, & p_6 = 0, \\
(3) & h_1 = -\lambda + a\sigma_1 + d\sigma_1^2, & h_3 = 1, \quad h_5 = 0, & p_2 = b\sigma_1 + cq - e, & p_4 = 1, & p_6 = 0,
\end{array}$$

where the following non-degeneracy conditions hold:

$$a + 1 \neq 0,\ 2a + 1 \neq 0,\ 3a + 1 \neq 0,\ 3b + 1 \neq 0, \text{ and } c \neq 0.$$

Because of the symmetry we see in certain models, we consider here another example.

**Lemma 2.7.** *Suppose that $g(\mathbf{z}, \lambda)$ has the form of (2.3) with*

$$h_1 = 2\lambda + a\sigma_1,\ h_3 = b,\ h_5 = 0,\ p_2 = e,\ p_4 = 0,\ p_6 = 0,$$

*and the non-degeneracy conditions $a+b \neq 0$, $2a+b \neq 0$, $3a+b \neq 0$, and $b \neq 0$. Then solving $g(\mathbf{z}, \lambda) = 0$ leads only to the following three types of nontrivial solutions:*

*(II) Rolls:* $x_1 = \sqrt{\frac{-2\lambda}{a+b}}$

*(III) Hexagons:* $x_1 = \frac{-e \pm \sqrt{e^2 - 8\lambda(3a+b)}}{2(3a+b)}$

*(IV) Rectangles:* $x_1 = \frac{e}{b}$ *and* $x_2 = \sqrt{\frac{-2\lambda b^2 - (a+b)e^2}{b^2(2a+b)}}$.

*The eigenvalues for the branches of solutions are given in Table 2.3.*

*Proof.* Using the reduced equations shown in Table 2.1, we will compute the various branches of solutions to $g(\mathbf{z}, \lambda) = 0$ which are exhibited in this case.

For solutions of type II (rolls), we are solving

$$0 = h_1 + x_1^2 h_3 + x_1^4 h_5 = 2\lambda + a\sigma_1 + bx_1^2.$$

Since $\sigma_1 = x_1^2$, we get $x_1 = \pm\sqrt{\frac{-2\lambda}{a+b}}$.

For hexagons, solutions of type III, we have that

$$\begin{aligned}
0 =& h_1 + x_1^2 h_3 + x_1^4 h_5 + x_1(p_2 + x_1^2 p_4 + x_1^4 p_6) \\
=& 2\lambda + a\sigma_1 + bx_1^2 + ex_1.
\end{aligned}$$

Table 2.3: Eigenvalues for each type of solution found in the case where $h_1 = 2\lambda + a\sigma_1$, $h_3 = b$, $h_5 = 0$, $p_2 = e$, $p_4 = 0$, and $p_6 = 0$.

| | Nomenclature | Eigenvalue | Multiplicity |
|---|---|---|---|
| I | Trivial | $2\lambda$ | 6 |
| II | Rolls | $2(a+b)x_1^2$ | 1 |
| | | $-ex_1 - bx_1^2$ | 2 |
| | | $ex_1 - bx_1^2$ | 2 |
| | | 0 | 1 |
| III | Hexagons | $3(a+b)x_1^2 - ex_1 + 2\lambda$ | 2 |
| | | $3(3a+b)x_1^2 + 2ex_1 + 2\lambda$ | 1 |
| | | $-3ex_1$ | 1 |
| | | 0 | 2 |
| IV | Rectangles | $2\lambda + ax_1^2 + (2a+3b)x_2^2 - ex_1$ | 1 |
| | | $2\lambda + (a+b)x_1^2 + 2ax_2^2 - 2ex_1$ | 1 |
| | | 0 | 2 |

and the eigenvalues of

$$\begin{bmatrix} 2\lambda + 3(a+b)x_1^2 + 2ax_2^2 & 4ax_1x_2 + 2ex_2 \\ 2ax_1x_2 + ex_2 & 2\lambda + ax_1^2 + 3(2a+b)x_2^2 + ex_1 \end{bmatrix}$$

Now $\sigma_1 = 3x_1^2$, so this leads to

$$x_1 = \frac{-e \pm \sqrt{e^2 - 8\lambda(3a+b)}}{2(3a+b)}.$$

Type IV solutions, rectangles, can be found by solving

$$\begin{aligned} 0 =& h_1 + x_2^2 h_3 + x_2^4 h_5 + x_1(p_2 + x_2^2 p_4 + x_2^4 p_6) \\ =& 2\lambda + a\sigma_1 + bx_2^2 + ex_1. \end{aligned}$$

In this case we have $\sigma_1 = x_1^2 + 2x_2^2$.There is another condition that

$$x_1[h_3 + (x_1^2 + x_2^2)h_5 + x_1 x_2^2 p_6] = p_2,$$

and this simplifies to $bx_1 = e$. Thus $x_1 = \frac{e}{b}$ and $x_2 = \pm\sqrt{\frac{-2\lambda b^2 - (a+b)e^2}{b^2(2a+b)}}$.

For solutions of type V, we have $H_1 = 0$ and $P_1 = 0$. Now $P_1 = e$, so type V solutions could only exist if $e = 0$. Since $u_1 = u_2 = u_3$, we have $\sigma_1 = 3u_1$, so the equation becomes $2\lambda + (3a+b)u_1 = 0$. Solving for $z_1$ gives $|z_1| = \sqrt{\frac{-2\lambda}{3a+b}}$. Since there are no other conditions, this solution is invariant under complex conjugation. Therefore, this solution is actually on the orbit of hexagons, type III, and there are no type V solutions.

Solutions of type VI and VIII both have conditions which reduce to $h_3 = 0$. Since $h_3 = b$ and $b \neq 0$ is one of the non-degeneracy conditions, we cannot have solutions of type VI or VIII in this example.

For solutions of type VII, we are solving the equations

$$x_j(h_1 + u_j h_3 + u_j^2 h_5) + x_\alpha x_\beta(p_2 + u_j p_4 + u_j^2 p_6) = 0$$

where $j = 1, 2, 3$ and $\alpha$ and $\beta$ are the other indices not equal to $j$. So the equations for $j = 1$ and $j = 2$ are respectively:

$$x_1(h_1 + u_1 h_3 + u_1^2 h_5) + x_2 x_3(p_2 + u_1 p_4 + u_1^2 p_6) = 0 \tag{2.17}$$

$$x_2(h_1 + u_2 h_3 + u_2^2 h_5) + x_1 x_3(p_2 + u_2 p_4 + u_2^2 p_6) = 0. \tag{2.18}$$

Now multiplying (2.17) by $x_1$ and multiplying (2.18) by $x_2$ and subtracting, and then dividing the result by $x_1^2 - x_2^2$ we get

$$2\lambda + a\sigma_1 + b(u_1 + u_2) = 0.$$

We can use a similar technique to get that

$$2\lambda + a\sigma_1 + b(u_1 + u_3) = 0$$

and

$$2\lambda + a\sigma_1 + b(u_2 + u_3) = 0.$$

Subtracting any one of these from another will give us that $u_1 = u_2 = u_3$, a contradiction. Thus, we do not have any solutions of type VII.

Hence the only nontrivial branches of solutions are those listed in the statement of the lemma. Now by computing the eigenvalues of $dg_{\mathbf{z}}(\mathbf{z}, \lambda)$ we can determine the stability of each of the branches of solutions. Since each of the branches of solutions are covered in Theorem 2.4, a direct application of its results gives the eigenvalues as listed in Table 2.3.

# Chapter 3

# Parlinski's model

In a series of papers [27, 28, 29, 30], Parlinski (along with several co-authors) studied several discrete models that showed incommensurate phases during phase transitions. Although most models were constructed on rectangular lattices, one such model [30] was defined on a hexagonal lattice. The authors mentioned quartz as one example of crystals that have hexagonal symmetry.

## 3.1 Definition and statement of the model

Parlinski's model [30] is proposed on a 2-D hexagonal lattice as shown in Figure 3.1. The lines in the lattice do not represent a bond between the atoms; they merely serve as a visual aid to show the periodicity of the lattice. We let the unit cell consist of $N \times N$ atoms and assume periodic boundary conditions since ideal crystals are infinite. The energy involves the interaction of each atom with its six nearest neighbors and six next-nearest neighbors. The energy function is written as

$$\begin{aligned} v = \frac{1}{2}\sum_{j,l}\{ & aX_{j,l}^2 + bX_{j,l}(X_{j+1,l} + X_{j-1,l} + X_{j,l+1} + X_{j,l-1} + X_{j+1,l+1} + X_{j-1,l-1}) \\ & + cX_{j,l}(X_{j+1,l-1} + X_{j-1,l+1} + X_{j+2,l+1} + X_{j-2,l-1} + X_{j+1,l+2} + X_{j-1,l-2}) \\ & + hX_{j,l}^3 + gX_{j,l}^4)\} \end{aligned} \tag{3.1}$$

where $X_{j,l}$ represents a displacement perpendicular to the plane of the lattice. The indices $j$ and $l$ are summed from 0 to $N-1$ so that each position in the unit cell is summed over exactly once.

The reciprocal lattice vectors $\mathbf{a}^*$ and $\mathbf{b}^*$ are defined so that $\mathbf{a}\cdot\mathbf{a}^* = 1$, $\mathbf{b}\cdot\mathbf{b}^* = 1$, $\mathbf{a}\cdot\mathbf{b}^* = 0$, and $\mathbf{b}\cdot\mathbf{a}^* = 0$.

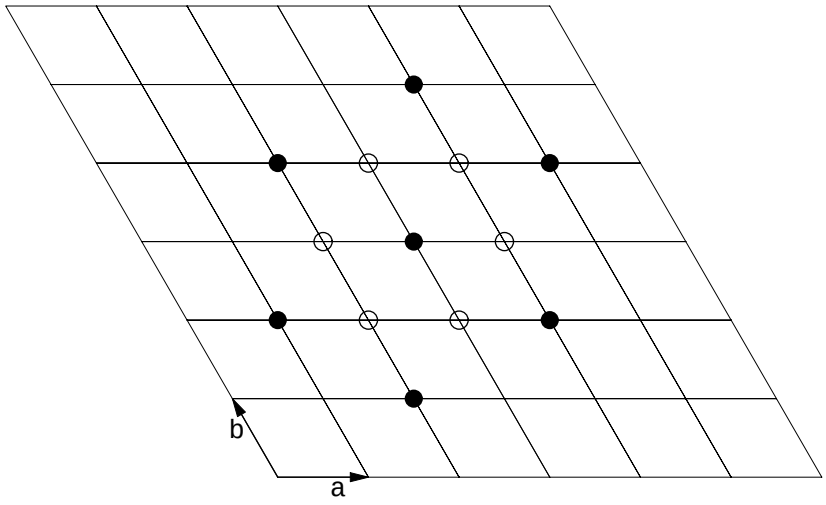


Figure 3.1: A hexagonal lattice showing the basis vectors **a** and **b**. Also shown are the six nearest neighbors (open circles) and six next-nearest neighbors (solid circles) of the center atom.

Some of the advantages of this model, in addition to its relative simplicity, are the positive fourth-order term which guarantees the existence of a stable solution and the third-order term which works along with the hexagonal symmetry to stabilize the 3q phase.

Another advantage for the modeling of quartz is that the phase diagram shows both commensurate and incommensurate 1q and 3q phases. We attempt now, along the lines of Parlinski, to compute the phase diagram for the model for a certain range of parameters.

## 3.2 Computational results

It is possible to rewrite (3.1) in dimensionless quantities, thus reducing the number of parameters from five to three. This is done by letting $X_0 = \sqrt{\frac{c}{g}}$ be the unit of length and $v_0 = \frac{c^2}{g}$ be the unit of energy. Then with the new parameters $A = \frac{a}{c}$, $B = \frac{b}{c}$, and $H = \frac{h}{\sqrt{cg}}$ and the new energy $V = \frac{v}{v_0}$, the energy function becomes

$$\begin{aligned} V = \frac{1}{2}\sum_{j,l}\{ & Ax_{j,l}^2 + Bx_{j,l}(x_{j+1,l} + x_{j-1,l} + x_{j,l+1} + x_{j,l-1} + x_{j+1,l+1} + x_{j-1,l-1}) \\ & + x_{j,l}(x_{j+1,l-1} + x_{j-1,l+1} + x_{j+2,l+1} + x_{j-2,l-1} + x_{j+1,l+2} + x_{j-1,l-2}) \\ & + Hx_{j,l}^3 + x_{j,l}^4)\}. \end{aligned} \tag{3.2}$$

Because of the reduced number of parameters, this form of the energy function is more useful in computing.

Parlinski's original paper [30] on this hexagonal model has as its main goal the computation of global minimizers of the energy for certain parameter values. This can be done using Newton's method. Because of the large number of local minimizers, it is necessary to determine some initial atomic arrangements that should be close to the global minimizers. This requires that we determine appropriate initial conditions near the global minimizer.

We assume that the global minimizer should take advantage of the symmetry of the lattice and the energy. This allows solutions which are modulated along one or more of the high symmetry directions. Solutions which display strip modulation are known as $1q$ while solutions which have a two-dimensional modulation are referred to as $3q$. We will see in the next section that $2q$ solutions are never stable, so they will not show up in our calculations of global minimizers.

In order for the modulation to fit to the size of the array of lattice points, we use periodic boundary conditions and expect the modulation to be periodic with period $N$ in each of the directions $\mathbf{a}$ and $\mathbf{b}$.

For the $1q$ modulation, the initial conditions are of the form $\cos(\frac{2\pi n}{N}\mathbf{a}^*)$, so one cosine wave is modulated along the direction of one of the reciprocal lattice vectors. For the $3q$ modulation,

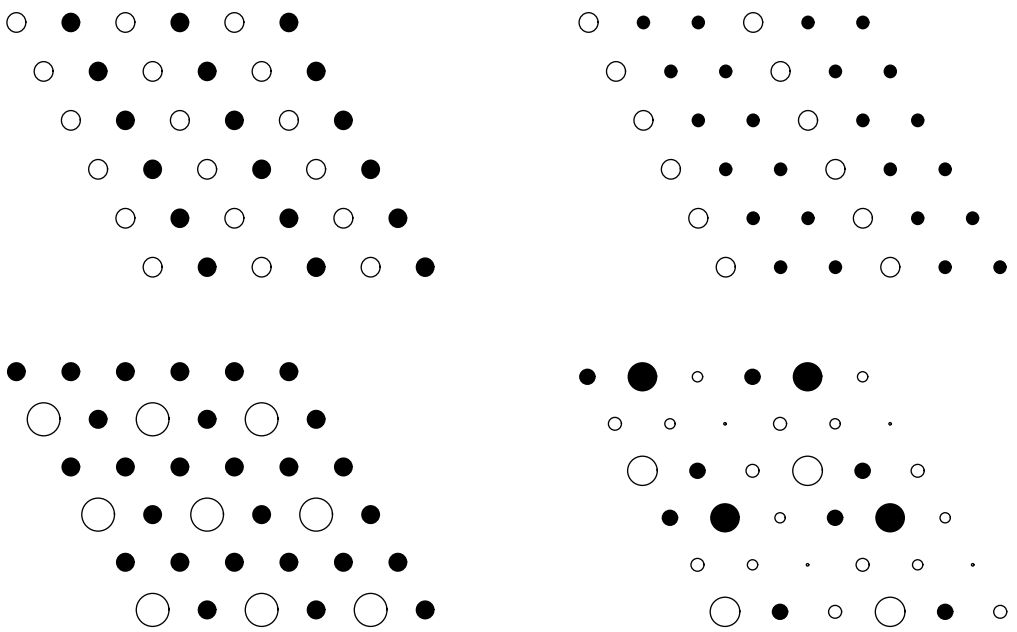

Figure 3.2: The displacements of atoms for commensurate $1q$ (top row) and $3q$ phases with modulation of $\frac{1}{2}$ (left column) and $\frac{1}{3}$. Open circles represent positive displacement, and filled circles represent negative displacement. The magnitude of the displacement is in proportion to the radius of the circle.

the initial conditions require cosine waves modulated along each of the high-symmetry directions of the reciprocal lattice. Typical configurations for $\frac{1}{2}$ and $\frac{1}{3}$ are shown in Figure 3.2 for both $1q$ and $3q$ conditions.

In their work, Parlinski *et al.* considered the phases with $\frac{M}{N} = \frac{0}{1}, \frac{1}{2}, \frac{1}{3}, \frac{1}{4}, \frac{1}{5}$, and $\frac{2}{5}$ to be commensurate phases. All other higher-order commensurate phases were treated as incommensurate phases because they produced the minimum energy in negligible regions of the phase diagram. Using these initial conditions in Newton's method produced the global minimizers of the energy as shown in Figure 3.3.

We observe several things from the computation of global minimizers. We notice that for modulation $\frac{1}{3}$, the $1q$ and $3q$ solutions are minimizers over the same region. This is because they reduce to the same energy. The configurations corresponding to the $\frac{1}{3}, 1q$ case are $x_{0,0}$ and $x_{1,0} = x_{2,0}$ in the unit strip. The unit cell of the $\frac{1}{3}, 3q$ case has $x_{0,0} = x_{1,0} = x_{1,1}$ and $x_{2,0} = x_{0,1} = x_{2,1} = x_{0,2} = x_{1,2} = x_{2,2}$. Substituting each of these conditions into (3.2) results in the same value for the energy.

We also see that when $H = 0$, we do not have any $3q$ solutions (except for the $\frac{1}{3}$ case

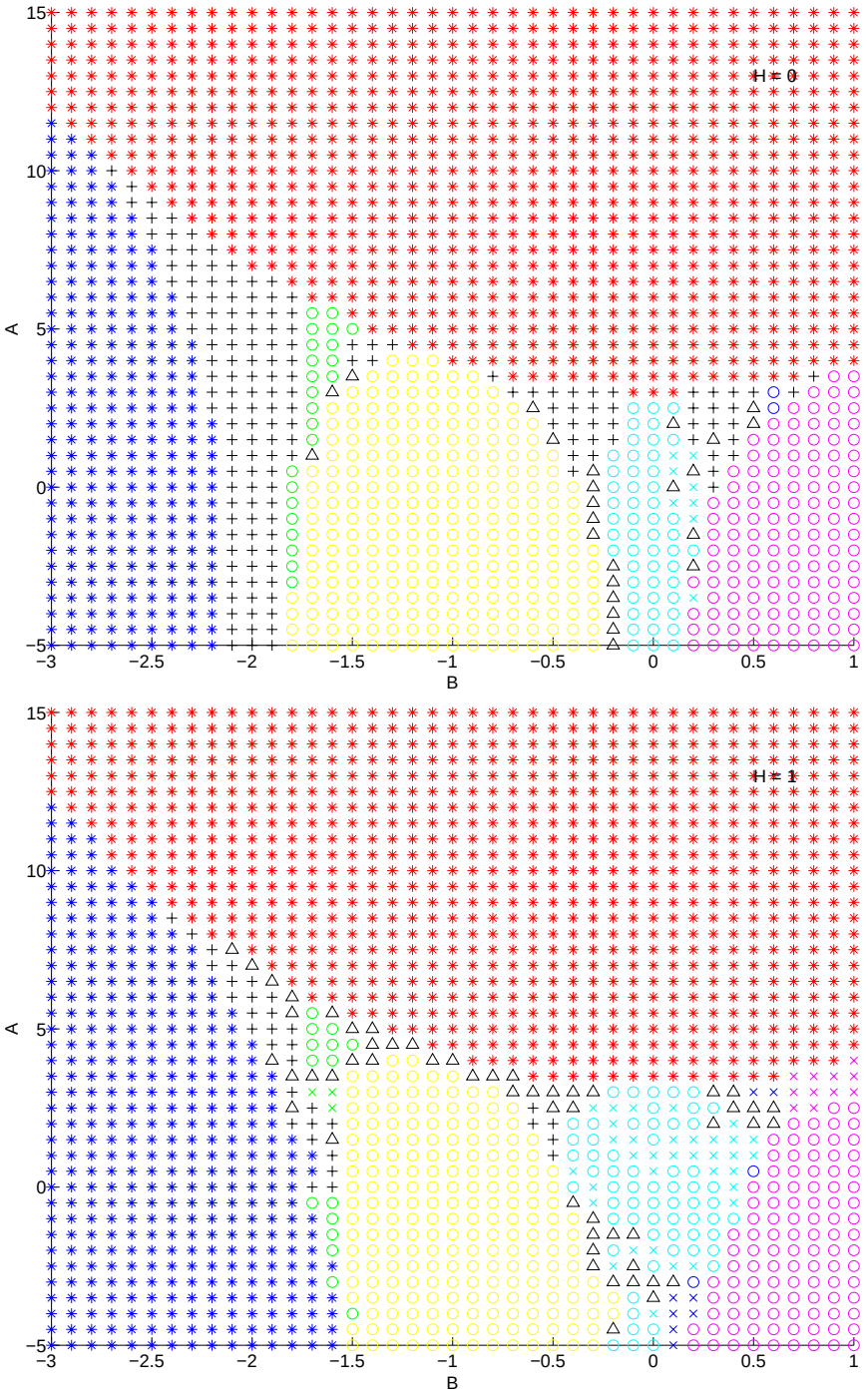


Figure 3.3: The ground state phase diagram for H=0 (top) and H=1. The red region corresponds to the normal (trivial) solution and the blue region corresponds to the $\mathbf{k} = 0$ region. The black + and $\triangle$ correspond to incommensurate 1q and 3q, respectively. The other color regions from left to right are $\frac{1}{5}$, $\frac{1}{4}$, $\frac{1}{3}$, $\frac{2}{5}$, $\frac{1}{2}$. The $\circ$ and $\times$ correspond to commensurate 1q and 3q, respectively.

mentioned above). We will discuss this more in the next section.

The picture appears much richer when $H \neq 0$. For the case $H = 1$, we see regions of both $1q$ and $3q$ commensurate and incommensurate regions. In order for a cooling run to move from the normal region to the commensurate $\mathbf{k} = 0$ region, it is necessary for A to decrease significantly while B and H change only slightly. In this type of experiment, the phase transition of the model would be normal $\rightarrow 3q \rightarrow 1q \rightarrow$ commensurate, $\mathbf{k} = 0$. For quartz, the normal phase would correspond to $\beta$-quartz while the $\mathbf{k} = 0$ phase corresponds to the $\alpha$-phase. This means that the incommensurate regions of this model are reached in reverse order of that of quartz, whose phase transition is believed to be $\beta \rightarrow 1q\ inc \rightarrow 3q\ inc \rightarrow \alpha$.

## 3.3 Energy in reciprocal space

While (3.2) was helpful for finding numerical solutions, in order to get analytical solutions, it is more useful to transfer the energy to reciprocal space. The reciprocal lattice vectors $\mathbf{a}^*$ and $\mathbf{b}^*$ are defined so that $\mathbf{a} \cdot \mathbf{a}^* = 1$, $\mathbf{b} \cdot \mathbf{b}^* = 1$, $\mathbf{a} \cdot \mathbf{b}^* = 0$, and $\mathbf{b} \cdot \mathbf{a}^* = 0$.

The tranformation of the energy to reciprocal space is done through a two-dimensional Fourier transformation. We let

$$x_{j,l} = \sum_{\mathbf{k}} z_{\mathbf{k}} e^{-i\mathbf{k}\cdot\mathbf{R}_{j,l}}$$

where $\mathbf{k} \cdot \mathbf{R}_{j,l} = (\frac{2\pi n}{N}\mathbf{a}^* + \frac{2\pi m}{N}\mathbf{b}^*) \cdot (j\mathbf{a} + l\mathbf{b}) = \frac{2\pi}{N}(nj + ml)$. The summation is taken to be over all reciprocal lattice vectors $\mathbf{k} = \frac{2\pi n}{N}\mathbf{a}^* + \frac{2\pi m}{N}\mathbf{b}^*$ where $n$ and $m$ are integers in the interval $(-\frac{N}{2}, \frac{N}{2}]$. For a thorough discussion of the reciprocal lattice, see [2].

Note that we can identify the set of $x$'s with a finite dimensional subspace of $\mathcal{F}^\Lambda$, defined in Section 2.1.

The inverse transformation is given by

$$z_{\mathbf{k}} = \sum_{j,l=0}^{N-1} x_{j,l} e^{i\mathbf{k}\cdot\mathbf{R}_{j,l}}.$$

Using this, we get that $z_{\mathbf{k}} = \bar{z}_{-\mathbf{k}}$ and $z_{\mathbf{k}+\mathbf{q}} = z_{\mathbf{k}}$ where $\mathbf{q}$ is any reciprocal lattice vector of the form $2\pi a_0\mathbf{a}^* + 2\pi b_0\mathbf{b}^*$ where $a_0$ and $b_0$ are any integers.

We will use the shorthand $W$ to represent $e^{-\frac{2\pi i}{N}}$ in this and future sections, and we prove the following lemma about $W$.

**Lemma 3.1.** *Let $W = e^{-\frac{2\pi i}{N}}$, $N \in \mathbb{N}$, and let $M$ be any integer. Then either $W^M = 1$ or $\sum_{k=-\frac{N}{2}+1}^{\frac{N}{2}} W^{Mk} = 0$. This means that we can write*

$$\sum_{k=-\frac{N}{2}+1}^{\frac{N}{2}} W^{Mk} = N\delta(\tfrac{M}{N} - \tau)$$

*where $\tau$ is an integer.*

*Proof.* Since $W = e^{-\frac{2\pi i}{N}}$, then $W^M = e^{-\frac{2\pi iM}{N}}$. Let $M$ be any integer. Then $W^{MN} = 1$. This means that

$$0 = W^{MN} - 1 = (W^M - 1)\sum_{k=0}^{N-1} W^{Mk}.$$

Therefore, if $M = 0, modN$, then $W^M = 1$, but if $M \neq 0, modN$, then $\sum_{k=0}^{N-1} W^{Mk} = 0$. The only way that $W^M$ can be 1 is for $\frac{M}{N}$ to be an integer. If it is true that $W^M = 1$, then taking the summation produces

$$\sum_{k=0}^{N-1} W^{Mk} = \sum_{k=0}^{N-1} 1^k = N.$$

Now we can see that

$$e^{-\frac{2\pi i}{N}(k-N)} = e^{-\frac{2\pi i}{N}k} e^{2\pi i} = e^{-\frac{2\pi i}{N}k}$$

so we can shift the index of the summation as follows:

$$\begin{aligned}
\sum_{k=0}^{N-1} W^k &= \sum_{k=0}^{N/2} W^k + \sum_{k=N/2+1}^{N-1} W^k \\
&= \sum_{k=0}^{N/2} W^k + \sum_{k=N/2+1}^{N-1} W^{k-N} \\
&= \sum_{k=0}^{N/2} W^k + \sum_{k=-N/2+1}^{-1} W^k \\
&= \sum_{k=-N/2+1}^{N/2} W^k.
\end{aligned}$$

Hence we have the stated summations. □

We always write the reciprocal lattice vectors as $\mathbf{k} = \frac{2\pi n}{N}\mathbf{a}^* + \frac{2\pi m}{N}\mathbf{b}^*$, so we can associate the vector $\mathbf{k}$ with the ordered pair $(n, m)$ and the vector $\mathbf{k}_\alpha$ with $(n_\alpha, m_\alpha)$. Now the transformation of each $x_{j,l}$ is written as

$$x_{j,l} = \sum_{\mathbf{k}} z_{\mathbf{k}} e^{-i\mathbf{k}\cdot\mathbf{R}_{j,l}} = \sum_{m,n=-N/2+1}^{N/2} z_{\mathbf{k}} W^{ml} W^{nj},$$

so that squaring the term produces

$$\begin{aligned}
x_{j,l}^2 &= (\sum_{\mathbf{k}_1} z_{\mathbf{k}_1} W^{m_1 l} W^{n_1 j})(\sum_{\mathbf{k}_2} z_{\mathbf{k}_2} W^{m_2 l} W^{n_2 j}) \\
&= \sum_{\mathbf{k}_1}\sum_{\mathbf{k}_2} z_{\mathbf{k}_1} z_{\mathbf{k}_2} W^{(m_1+m_2)l} W^{(n_1+n_2)j}.
\end{aligned}$$

Then taking the summation over all $j$ and $l$, we get

$$\sum_{j,l} x_{j,l}^2 = \sum_{\mathbf{k}_1}\sum_{\mathbf{k}_2} z_{\mathbf{k}_1} z_{\mathbf{k}_2} \sum_{l=0}^{N-1} W^{(m_1+m_2)l} \sum_{j=0}^{N-1} W^{(n_1+n_2)j},$$

and we can eliminate the sums over $j$ and $l$ on the right-hand side using the following lemma.

Hence the transformation of the first term of the energy would look like

$$\sum_{j,l} x_{j,l}^2 = N^2 \sum_{\mathbf{k}_1}\sum_{\mathbf{k}_2} z_{\mathbf{k}_1} z_{\mathbf{k}_2} \delta(\frac{m_1+m_2}{N} - \tau_1)\delta(\frac{n_1+n_2}{N} - \tau_2),$$

where $\tau_1$ and $\tau_2$ are integers.

Other terms in the energy involve interactions between two neighboring atoms. These are denoted by subscripts such as $j+1$ or $l-2$, for example. To accomodate for all of these, suppose that $p$ and $r$ are elements of the set $\{-2,-1,0,1,2\}$. Then we can write all of the nearest and next-nearest neighbor interactions as $x_{j,l}x_{j+p,l+r}$. Now

$$\begin{aligned} x_{j,l}x_{j+p,l+r} &= (\sum_{\mathbf{k}_1} z_{\mathbf{k}_1} W^{m_1 l} W^{n_1 j})(\sum_{\mathbf{k}_2} z_{\mathbf{k}_2} W^{m_2(l+r)} W^{n_2(j+p)}) \\ &= \sum_{\mathbf{k}_1}\sum_{\mathbf{k}_2} z_{\mathbf{k}_1} z_{\mathbf{k}_2} W^{(m_1+m_2)l} W^{(n_1+n_2)j} W^{pn_2+rm_2}, \end{aligned}$$

so that the summation over $j$ and $l$ becomes

$$\begin{aligned} \sum_{j,l} x_{j,l}x_{j+p,l+r} &= \sum_{\mathbf{k}_1}\sum_{\mathbf{k}_2} z_{\mathbf{k}_1} z_{\mathbf{k}_2} W^{pn_2+rm_2} \sum_{l=0}^{N-1} W^{(m_1+m_2)l} \sum_{j=0}^{N-1} W^{(n_1+n_2)j} \\ &= N^2 \sum_{\mathbf{k}_1}\sum_{\mathbf{k}_2} z_{\mathbf{k}_1} z_{\mathbf{k}_2} W^{pn_2+rm_2} \delta(\frac{m_1+m_2}{N} - \tau_1)\delta(\frac{n_1+n_2}{N} - \tau_2). \end{aligned}$$

Notice that

$$W^{pn_2+rm_2} = e^{-\frac{2\pi i}{N}(pn_2+rm_2)} = \cos(2\pi\frac{pn_2+rm_2}{N}) - i\sin(2\pi\frac{pn_2+rm_2}{N}).$$

In a manner similar to that above, we can see that the transformations of the higher order terms looks like

$$\begin{aligned} \sum_{j,l} x_{j,l}^3 &= N^2 \sum_{\mathbf{k}_1}\sum_{\mathbf{k}_2}\sum_{\mathbf{k}_3} z_{\mathbf{k}_1} z_{\mathbf{k}_2} z_{\mathbf{k}_3} \delta(\frac{m_1+m_2+m_3}{N} - \tau_1)\delta(\frac{n_1+n_2+n_3}{N} - \tau_2) \\ \sum_{j,l} x_{j,l}^4 &= N^2 \sum_{\mathbf{k}_1}\sum_{\mathbf{k}_2}\sum_{\mathbf{k}_3}\sum_{\mathbf{k}_4} z_{\mathbf{k}_1} z_{\mathbf{k}_2} z_{\mathbf{k}_3} z_{\mathbf{k}_4} \delta(\frac{m_1+m_2+m_3+m_4}{N} - \tau_1)\delta(\frac{n_1+n_2+n_3+n_4}{N} - \tau_2) \end{aligned}$$

This results in the energy (3.2) becoming

$$\begin{aligned} V = \frac{N^2}{2}\Big\{ &\sum_{\mathbf{k}_1}\sum_{\mathbf{k}_2} \omega^2(n_1,m_1) z_{\mathbf{k}_1} z_{\mathbf{k}_2} \delta(\tfrac{m_1+m_2}{N} - \tau_1)\delta(\tfrac{n_1+n_2}{N} - \tau_2) \\ &+ H\sum_{\mathbf{k}_1}\sum_{\mathbf{k}_2}\sum_{\mathbf{k}_3} z_{\mathbf{k}_1} z_{\mathbf{k}_2} z_{\mathbf{k}_3} \delta(\tfrac{m_1+m_2+m_3}{N} - \tau_3)\delta(\tfrac{n_1+n_2+n_3}{N} - \tau_4) \\ &+ \sum_{\mathbf{k}_1}\sum_{\mathbf{k}_2}\sum_{\mathbf{k}_3}\sum_{\mathbf{k}_4} z_{\mathbf{k}_1} z_{\mathbf{k}_2} z_{\mathbf{k}_3} z_{\mathbf{k}_4} \delta(\tfrac{m_1+m_2+m_3+m_4}{N} - \tau_5)\delta(\tfrac{n_1+n_2+n_3+n_4}{N} - \tau_6)\Big\}. \end{aligned} \tag{3.3}$$

where the dispersion function $\omega^2(n,m)$ is given by

$$\begin{aligned} \omega^2(n,m) =& A + 2B[\cos 2\pi\frac{n}{N} + \cos 2\pi\frac{m}{N} + \cos 2\pi\frac{n+m}{N}] \\ &+ 2[\cos 2\pi\frac{n-m}{N} + \cos 2\pi\frac{2n+m}{N} + \cos 2\pi\frac{n+2m}{N}]. \end{aligned} \tag{3.4}$$

Even though we write the dispersion function as $\omega^2$, it is possible for it to become negative.

In order to avoid repeating $N^2$ in all of the remaining references to the energy or its derivatives, we will use a new energy function $V = \frac{1}{N^2}V$.

We are interested in finding equilibrium solutions of $\ddot{z} = -\nabla_z V$ which bifurcate from the trivial solution. The implicit function theorem tells us that the trivial solution is "locally unique" if the eigenvalues of the Hessian matrix of $V$ are all positive. These eigenvalues are given by the values of the dispersion function, so these are all positive if $A$ is sufficiently large.

We wish to examine the smallest eigenvalue of the Hessian which corresponds to the smallest value of $\omega^2(n,m)$ for $\mathbf{k} = \frac{2\pi n}{N}\mathbf{a}^* + \frac{2\pi m}{N}\mathbf{b}^*$ where $n$ and $m$ are integers in the interval $(-\frac{N}{2}, \frac{N}{2}]$. By symmetry we see that in general

$$\begin{aligned} \omega^2(n,m) = \omega^2(-n,-m) = \omega^2(m,n) = \omega^2(-m,-n) \\ =\omega^2(n,-n-m) = \omega^2(-n,n+m) = \omega^2(n+m,-n) = \omega^2(-n-m,n) \\ =\omega^2(m,-n-m) = \omega^2(-m,n+m) = \omega^2(n+m,-m) = \omega^2(-n-m,m), \end{aligned}$$

so the smallest eigenvalue could have a 12-dimensional eigenspace. However, along the high symmetry directions $a^*$, $b^*$, $b^* - a^*$, and the opposites of these, we have

$$\begin{aligned} \omega^2(n,0) = \omega^2(-n,0) = \omega^2(0,n) = \omega^2(0,-n) \\ = \omega^2(n,-n) = \omega^2(-n,n), \end{aligned}$$

so there is a 6-dimensional eigenspace. Since there are only finite choices for $n$ and $m$ given $N$, it is easy to check that the smallest eigenvalue has this form for a particular $A$ and $B$. (Parlinski assumes this form for the smallest eigenvalue.)

Let the six reciprocal lattice vectors at which the dispersion function is minimized be given by $\mathbf{k}_1, \mathbf{k}_2, \ldots, \mathbf{k}_6$, where $\mathbf{k}_1+\mathbf{k}_2+\mathbf{k}_3 = 0$ and $\mathbf{k}_j = -\mathbf{k}_{j+3}$ for $j = 1, 2, 3$. Denote the amplitudes corresponding to $\mathbf{k}_1, \ldots, \mathbf{k}_6$ by $z_1, \ldots, z_6$ and notice that $z_j = \bar{z}_{j+3}$ for $j = 1, 2, 3$.

We now search for approximate equilibrium solutions involving these six amplitudes only. For such solutions, the energy reduces to

$$\begin{aligned}\tilde{V} =& \tfrac{1}{2}\{2\lambda(|z_1|^2 + |z_2|^2 + |z_3|^2) + 6H(z_1z_2z_3 + \bar{z}_1\bar{z}_2\bar{z}_3) + 6(|z_1|^4 + |z_2|^4 + |z_3|^4) \\ &+ 24(|z_1|^2|z_2|^2 + |z_1|^2|z_3|^2 + |z_2|^2|z_3|^2)\}\end{aligned} \tag{3.5}$$

where $\lambda$ is the value of the dispersion function.

Now using the approximation (3.5), $\nabla\tilde{V}$ is of the form

$$\nabla_{\mathbf{z}}\tilde{V} = g(\mathbf{z}) = \begin{pmatrix} 2\lambda z_1 + 6H\bar{z}_2\bar{z}_3 + 12z_1|z_1|^2 + 24z_1(|z_2|^2 + |z_3|^2) \\ 2\lambda z_2 + 6H\bar{z}_1\bar{z}_3 + 12z_2|z_2|^2 + 24z_2(|z_1|^2 + |z_3|^2) \\ 2\lambda z_3 + 6H\bar{z}_1\bar{z}_2 + 12z_3|z_3|^2 + 24z_3(|z_2|^2 + |z_2|^2) \end{pmatrix}.$$

Note that $g(\mathbf{z})$ is simply six components of the gradient of the full energy, $\nabla_{\mathbf{z}}V$. In solving $g(\mathbf{z}) = 0$ we are solving these components of $\nabla_{\mathbf{z}}V = 0$ exactly. The remaining $N^2 - 6$ components of $\nabla_{\mathbf{z}}V$ are of order $\epsilon^2$ where $\epsilon$ is the amplitude of the solution of $g(\mathbf{z}) = 0$.

We can rewrite $g(\mathbf{z})$ to match the notation of Golubitsky from the previous chapter by writing it as

$$g(\mathbf{z}) = \begin{pmatrix} z_1(2\lambda + 12|z_1|^2 + 24|z_2|^2 + 24|z_3|^2) + \bar{z}_2\bar{z}_3(6H) \\ z_2(2\lambda + 12|z_2|^2 + 24|z_1|^2 + 24|z_3|^2) + \bar{z}_1\bar{z}_3(6H) \\ z_3(2\lambda + 12|z_3|^2 + 24|z_1|^2 + 24|z_2|^2) + \bar{z}_1\bar{z}_2(6H) \end{pmatrix}.$$

Here we have $g(\mathbf{z})$ in the form (2.3) where $H_j = h_1 + u_jh_3 + u_j^2h_5$ and $K_j = k_2 + u_jk_4 + u_j^2k_6$. For Parlinski's model, $h_1 = 2\lambda + 24\sigma_1$, $h_3 = -12$, $h_5 = 0$, $k_2 = 6H$, $k_4 = 0$, and $k_6 = 0$. Recall that $\sigma_1 = |z_1|^2 + |z_2|^2 + |z_3|^2$. This case is covered by our extension of Golubitsky's results discussed in section 2.4, so we can directly apply the results from that section.

The solutions that we get for this model are

| | | |
|---|---|---|
| (II) | Rolls: | $x_1 = \pm\sqrt{\frac{-\lambda}{6}}$ |
| (III$^+$) | Hexagons: | $x_1 = \frac{1}{60}(-3H + \sqrt{9H^2 - 120\lambda})$ |
| (III$^-$) | Hexagons: | $x_1 = \frac{1}{60}(-3H - \sqrt{9H^2 - 120\lambda})$ |
| (IV) | Rectangles: | $x_1 = \frac{-H}{2}$ and $x_2 = \pm\frac{1}{6}\sqrt{-3H^2 - 2\lambda}$. |

Recall that there are two orbits of hexagons. We will denote these with a + or − sign which corresponds to the sign of $x_1$. Also notice that the rectangles are only possible when $\lambda < -\frac{3}{2}H^2$. This means that for $H \neq 0$, the bifurcation at $\lambda = 0$ will not include this solution. This branch will be a secondary bifurcation.

We can also easily compute the stability of the solutions using the results of section 2.3. Substituting the values into the eigenvalues from Table 2.4 gives the eigenvalues for the various branches of solutions. These are shown in Table 3.3.

Table 3.1: Eigenvalues for each type of solution in Parlinski's model.

| | Nomenclature | Eigenvalue | Multiplicity |
|---|---|---|---|
| I | Trivial | $2\lambda$ | 6 |
| II | Rolls | $-4\lambda$ | 1 |
| | | $-2\lambda - H\sqrt{-6\lambda}$ | 2 |
| | | $-2\lambda + H\sqrt{-6\lambda}$ | 2 |
| | | $0$ | 1 |
| $III^+$ | Hexagons$^+$ | $\frac{4}{25}(5\lambda + 3H^2 - H\sqrt{9H^2 - 120\lambda})$ | 2 |
| | | $\frac{1}{10}(-40\lambda + 3H^2 - H\sqrt{9H^2 - 120\lambda})$ | 1 |
| | | $\frac{3}{10}(3H^2 - H\sqrt{9H^2 - 120\lambda})$ | 1 |
| | | $0$ | 2 |
| $III^-$ | Hexagons$^-$ | $\frac{4}{25}(5\lambda + 3H^2 + H\sqrt{9H^2 - 120\lambda})$ | 2 |
| | | $\frac{1}{10}(-40\lambda + 3H^2 + H\sqrt{9H^2 - 120\lambda})$ | 1 |
| | | $\frac{3}{10}(3H^2 + H\sqrt{9H^2 - 120\lambda})$ | 1 |
| | | $0$ | 2 |
| IV | Rectangles | $\frac{4}{3}\lambda + 8H^2$ | 1 |
| | | $\frac{-2}{3}\lambda + 5H^2$ | 1 |
| | | $0$ | 2 |
| | | $\frac{1}{6}(-14\lambda - 3H^2 + \sqrt{-855H^4 - 636H^2\lambda + 100\lambda^2})$ | 1 |
| | | $\frac{1}{6}(-14\lambda - 3H^2 - \sqrt{-855H^4 - 636H^2\lambda + 100\lambda^2})$ | 1 |

All of the eigenvalues in the table are real. Since the problem that we are solving is $\ddot{\mathbf{z}} = -g(\mathbf{z})$, the solutions are stable when the eigenvalues are positive. It is then immediately obvious that the trivial solution is stable when $\lambda > 0$ and unstable when $\lambda < 0$. Since there are zero eigenvalues for each of the nontrivial branches of solutions, we can look at higher order derivatives to determine their stability.

Before we do this, it is rather easy to verify Parlinski's claim that the $2q$ solutions (rectangles) are never stable. Because $x_2$ is real and $x_2 = \pm\frac{1}{6}\sqrt{-3H^2 - 2\lambda}$, it is necessary that $\lambda < -\frac{3}{2}H^2$ for the solution to exist. The first eigenvalue for rectangles listed in Table 3.3 is $\frac{4}{3}\lambda + 8H^2$. This must be greater than 0 in order for the solution to be stable, so this requires that $\lambda > -6H^2$. Now consider the last eigenvalue for rectangles, $\frac{1}{6}(-14\lambda - 3H^2 - \sqrt{-855H^4 - 636H^2\lambda + 100\lambda^2})$. If this eigenvalue is greater than zero, then $14\lambda - 3H^2 > \sqrt{-855H^4 - 636H^2\lambda + 100\lambda^2}$. (Notice that the left-hand side will always be positive since $\lambda < -\frac{3}{2}H^2$.) Squaring both sides of the inequality, combining terms, and factoring out 48 gives us $2\lambda^2 + 15H^2\lambda + 18H^4 > 0$. By factoring, this reduces to $(2\lambda + 3H^2)(\lambda + 6H^2) > 0$. In order for this to be satisfied, either $\lambda > -\frac{3}{2}H^2$ or $\lambda < -6H^2$. These are the opposites of the previous stated inequalities, so there is no region where rectangles will be stable.

For rolls, we have $x_1 = -\sqrt{\frac{-\lambda}{6}}$. Since $x_1$ is real, rolls only exist when $\lambda < 0$. This means that the first eigenvalue is positive. If the second eigenvalue is positive, then $-2\lambda > H\sqrt{-6\lambda}$. This is clear if $H \leq 0$, so assume $H > 0$. Then squaring both sides and dividing by $4\lambda$ results in $\lambda < -\frac{3}{2}H^2$. Similarly, the third eigenvalue being positive implies that $-2\lambda > -H\sqrt{-6\lambda}$ which is clear if $H \geq 0$. Now assuming that $H < 0$ and squaring both sides results in $\lambda < -\frac{3}{2}H^2$. So all of the nonzero eigenvalues are positive as long as $\lambda < -\frac{3}{2}H^2$, but one of them is negative if $\lambda > -\frac{3}{2}H^2$. So rolls are unstable if $\lambda > -\frac{3}{2}H^2$, but we must examine the zero eigenvalue to say anything more.

The hexagon solutions are $x_1 = \frac{-3H \pm \sqrt{9H^2 - 120\lambda}}{60}$. Since this is real, it must be that $\lambda < \frac{3}{40}H^2$. If we only consider that $\lambda < 0$, then we have that $\sqrt{9H^2 - 120\lambda} > \sqrt{9H^2} = 3H\text{sgn}(H)$. The two types of hexagons have opposite stability, depending on the sign of the parameter $H$. Consider this for the third eigenvalue listed for the hexagon solutions:

$$\frac{3}{10}(3H^2 - H\text{sgn}(H)\sqrt{9H^2 - 120\lambda}) < \frac{3}{10}(3H^2 - H\text{sgn}(H)(3H\text{sgn}(H))) = 0.$$

This means that III$^+$ solutions will be unstable if $H > 0$ and III$^-$ solutions will be unstable if $H < 0$.

Setting the first eigenvalue equal to zero and simplifying the equation, we get

$$5\lambda + 3H^2 = \pm H\sqrt{9H^2 - 120\lambda},$$

where H is positive for III$^-$ solutions and negative for III$^+$ solutions. Squaring both sides and solving for $\lambda$, we get that either $\lambda = 0$ or $\lambda = -6H^2$. Thus the eigenvalue is positive if $-6H^2 < \lambda < 0$. The other eigenvalue is positive in this region also, so we need to study the zero eigenvalue to determine the actual region of stability.

In order to consider the zero eigenvalues, we must consider higher order derivatives. From $g(\mathbf{z})$ given in (3.6), we can calculate $dg(\mathbf{z})$ for rolls and hexagons in order to determine the eigenvector associated with the zero eigenvalue. We will write $g$ in real coordinates as was done in (2.8), and will calculate $dg_{(x,y)}$.

For rolls, we have that

$$dg(\sqrt{\frac{-\lambda}{6}},0,0,0,0,0) = \begin{bmatrix} -4\lambda & 0 & 0 & 0 & 0 & 0 \\ 0 & -2\lambda & H\sqrt{-6\lambda} & 0 & 0 & 0 \\ 0 & H\sqrt{-6\lambda} & -2\lambda & 0 & 0 & 0 \\ 0 & 0 & 0 & 0 & 0 & 0 \\ 0 & 0 & 0 & 0 & -2\lambda & -H\sqrt{-6\lambda} \\ 0 & 0 & 0 & 0 & -H\sqrt{-6\lambda} & -2\lambda \end{bmatrix},$$

so the zero eigenvalue is $(0,0,0,1,0,0)$, so we need to consider higher order derivatives with respect to $y_1$. Evaluating the derivatives at the solutions for rolls, we get that $\frac{\partial^3 \tilde{V}}{\partial y_1^3} = 72y_1 = 0$ and $\frac{\partial^4 \tilde{V}}{\partial y_1^4} = 72 > 0$. Thus the rolls are stable on the region found above, namely $\lambda < -\frac{3}{2}H^2$.

The matrix $dg$ for hexagons is written in real coordinates as

$$dg(\mathbf{z}) = \begin{bmatrix} 2\lambda+84x_1^2 & 6Hx_1+48x_1^2 & 6Hx_1+48x_1^2 & 0 & 0 & 0 \\ 6Hx_1+48x_1^2 & 2\lambda+84x_1^2 & 6Hx_1+48x_1^2 & 0 & 0 & 0 \\ 6Hx_1+48x_1^2 & 6Hx_1+48x_1^2 & 2\lambda+84x_1^2 & 0 & 0 & 0 \\ 0 & 0 & 0 & 2\lambda+60x_1^2 & -6Hx_1 & -6Hx_1 \\ 0 & 0 & 0 & -6Hx_1 & 2\lambda+60x_1^2 & -6Hx_1 \\ 0 & 0 & 0 & -6Hx_1 & -6Hx_1 & 2\lambda+60x_1^2 \end{bmatrix}$$

where $\mathbf{z} = (x_1, x_1, x_1, 0, 0, 0)$ and $x_1 = \frac{1}{60}(-3H \pm \sqrt{9H^2 - 120\lambda})$. For each of these two values of $x_1$, we have that $2\lambda + 60x_1^2 = -6Hx_1$. This means that the lower right $3\times3$ submatrix has the same entries in each position, so the zero eigenvalues correspond to the eigenvectors $(0,0,0,-1,0,1)$ and $(0,0,0,-1,1,0)$. A linear combination of these vectors can be written as $u = a(0,0,0,-1,0,1) + b(0,0,0,-1,1,0)$ where $a$ and $b$ are constants. Then we can find the partial derivatives of $\tilde{V}$ along any such vector $u$. This can be done as

$$\sum_{i,j,k=1}^{3} u_{i+3}u_{j+3}u_{k+3}\frac{\partial^3 \tilde{V}}{\partial y_i \partial y_j \partial y_k}.$$

Notice that any third partial of $\tilde{V}$ with repect to the $y$ variables evaluated at $y = 0$ will be zero. The fourth partial of $\tilde{V}$ along the direction $u$ is given by

$$\sum_{i,j,k,l=1}^{3} u_{i+3}u_{j+3}u_{k+3}u_{l+3}\frac{\partial^4 \tilde{V}}{\partial y_i \partial y_j \partial y_k \partial y_l}$$
$$= 72a^4 + 288a^2(a+b)^2 + 72(a+b)^4 + 288a^2b^2 + 288(a+b)^2b^2 + 72b^4.$$

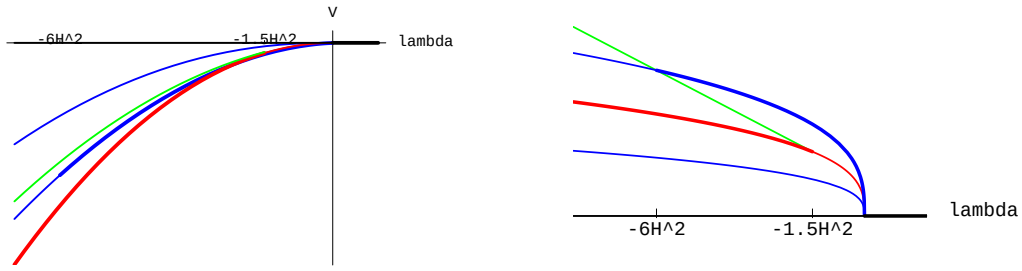


Figure 3.4: The bifurcation diagram of Parlinski's model. The red, green, and blue curves correspond to the $1q$, $2q$, and $3q$ solutions, respectively. Stable solutions are shown as thick curves while unstable solutions are thin. The left picture shows the energy of the various solutions versus the bifurcation parameter $\lambda$. The graph on the right is a magnification to better show the various solutions.

It is easy to see that this is always positive. Thus the hexagons are stable on the region found above, namely if $-6H^2 < \lambda < 0$, then III$^+$ is stable when $H < 0$ and III$^-$ is stable when $H > 0$.

Thus the bifurcation picture has the trivial solution as the only stable branch for $\lambda > 0$. Then at $\lambda = 0$, there are three new branches - one for rolls and two for hexagons. One of the hexagon branches will be the only stable solution on the region $-\frac{3}{2}H^2 < \lambda < 0$. Then the rolls become stable. Also at $\lambda = -\frac{3}{2}H^2$, another branch of solutions (rectangles) appears, although it never becomes stable. Then at $\lambda = -6H^2$, the hexagons lose their stability, so that rolls are the only stable branch for $\lambda < -6H^2$.

Plugging the solutions into the energy function (3.5) gives the following energy for the various branches of solutions:

(II) Rolls: $\tilde{V} = -\frac{\lambda^2}{12}$

(III$^+$) Hexagons: $\tilde{V} = \frac{1}{12000}(-9H^4 + 180H^2\lambda - 600\lambda^2 + (3H^3 - 40H)\sqrt{9H^2 - 120\lambda})$

(III$^-$) Hexagons: $\tilde{V} = \frac{1}{12000}(-9H^4 + 180H^2\lambda - 600\lambda^2 - (3H^3 - 40H)\sqrt{9H^2 - 120\lambda})$

(IV) Rectangles: $\tilde{V} = \frac{1}{144}(9H^4 + 12H^2\lambda - 8\lambda^2)$.

By setting the energy for the rolls equal to the energy for the hexagons and solving for $\lambda$, we can determine which has the lowest energy. Doing this, we find that the energy for rolls is the minimum energy when $\lambda < -\frac{3}{20}(7 + 3\sqrt{6})H^2$. This is approximately $-2.15H^2$. Thus the rolls and one branch of hexagons will be stable over the region $-6H^2 < \lambda < -\frac{3}{2}H^2$, and the minimum energy will change solution type at $-\frac{3}{20}(7 + 3\sqrt{6})H^2$.

## 3.4 Conclusions

Parlinski's model originally showed much promise for modeling quartz. It has the correct symmetry and includes both $1q$ and $3q$ inc phases. However, as was shown in both the computational and analytical solutions, the phase transition of the model on cooling is $\beta \rightarrow 3q\ inc \rightarrow 1q\ inc \rightarrow \alpha$ while the actual transition of quartz is $\beta \rightarrow 1q\ inc \rightarrow 3q\ inc \rightarrow \alpha$. Hence we agree with Parlinski's assessment that this model cannot be applied to quartz directly.

In the next chapter, we address the question of whether appropriate modifications can be made to Parlinski's model which would allow it to follow the transition of quartz correctly.

# Chapter 4

# Modifying Parlinski's Model

Since Parlinski's hexagonal model does not exhibit the correct sequence in phase transition, it is natural to ask if modifications to the model can be made in order to attain the correct sequence. The unfortunate answer is "no." In this chapter we will propose several different modifications to the original model, and we will show how all such modifications eventually reduce to essentially the same energy function through the discrete Fourier transform into reciprocal space.

## 4.1 Modifications to the cubic term

Any modification should naturally keep the hexagonal symmetry of the lattice, and it seems productive to keep the interactions between nearest and next-nearest neighbors. We will begin by making modifications to the cubic term of the original energy.

Recall that after the change to dimensionless quantities, the energy function was

$$\begin{aligned} V = \frac{1}{2}\sum_{j,l}\{&Ax_{j,l}^2 + Bx_{j,l}(x_{j+1,l} + x_{j-1,l} + x_{j,l+1} + x_{j,l-1} + x_{j+1,l+1} + x_{j-1,l-1}) \\ &+ x_{j,l}(x_{j+1,l-1} + x_{j-1,l+1} + x_{j+2,l+1} + x_{j-2,l-1} + x_{j+1,l+2} + x_{j-1,l-2}) \\ &+ Hx_{j,l}^3 + x_{j,l}^4)\}. \end{aligned} \tag{4.1}$$

We begin by modifying the cubic term $x_{j,l}^3$ to include interactions between nearest neighbors in the hope that doing so will change the order of the transition of the model to that of quartz.

Although others are certainly possible, we will describe two possible additions to the cubic

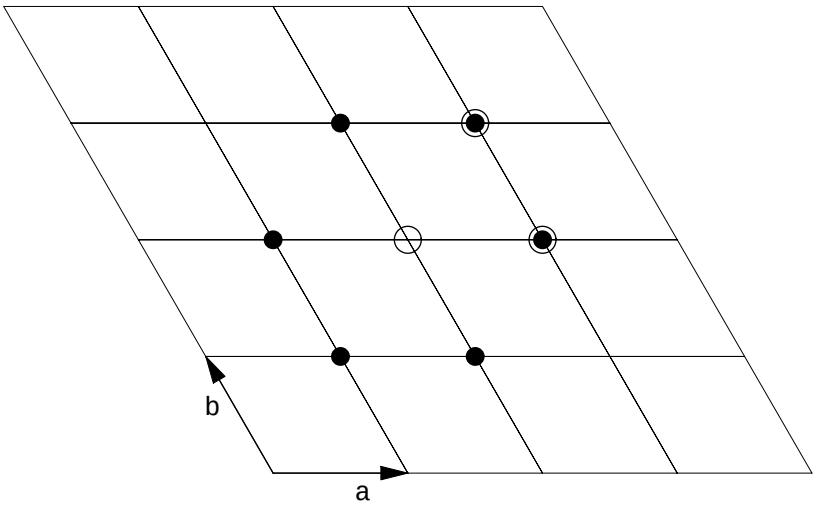


Figure 4.1: A possible modification to the cubic term of the energy. The three atoms with open circles are one term of (4.4). The other terms are obtained by rotations of 60°.

term, and we introduce new parameters in the process.

$$Cx_{j,l}^2(x_{j+1,l} + x_{j-1,l} + x_{j,l+1} + x_{j,l-1} + x_{j+1,l+1} + x_{j-1,l-1}) \tag{4.2}$$

$$\begin{aligned} Dx_{j,l}(&x_{j+1,l}x_{j,l-1} + x_{j,l-1}x_{j-1,l-1} + x_{j-1,l-1}x_{j-1,l} \\ &+x_{j-1,l}x_{j,l+1} + x_{j,l+1}x_{j+1,l+1} + x_{j+1,l+1}x_{j+1,l}) \end{aligned} \tag{4.3}$$

It is easy to see that (4.2) is just the interaction with the nearest neighbors, similar to a piece of the quadratic part of the energy, but squaring the center atom. Notice that a term of the form

$$Cx_{j,l}(x_{j+1,l}^2 + x_{j-1,l}^2 + x_{j,l+1}^2 + x_{j,l-1}^2 + x_{j+1,l+1}^2 + x_{j-1,l-1}^2)$$

is the same as (4.2) because we are summing over all elements of the lattice.

In (4.4), the interaction is between a triple of nearest neighbors. As you can see in Figure 4.1, we merely focus on the central atom and multiply it by two atoms which are nearest neighbors of each other as well as nearest neighbors of the central atom.

In this way, we have enumerated all of the possible cubic interactions which involve nearest neighbors only. If we were to include next-nearest neighbors also, the list of possible cubic interactions would increase dramatically. This is not a problem however, because we will eventually show a general result for any number of neighbors.

Recall that in doing the discrete Fourier transform as in (3.3), we use

$$x_{j,l} = \sum_{\mathbf{k}} z_{\mathbf{k}} e^{-i\mathbf{k}\cdot\mathbf{R}_{j,l}}$$

where $\mathbf{k}\cdot\mathbf{R}_{j,l} = (\frac{2\pi n}{N}\mathbf{a}^* + \frac{2\pi m}{N}\mathbf{b}^*)\cdot(j\mathbf{a}+l\mathbf{b}) = \frac{2\pi}{N}(nj+ml)$. Throughout this section and the rest of the chapter, we use the notation $\mathbf{k} = \frac{2\pi n}{N}\mathbf{a}^* + \frac{2\pi m}{N}\mathbf{b}^*$, so we can associate the vector $\mathbf{k}$ with the ordered pair $(n,m)$ and the vector $\mathbf{k}_\alpha$ with $(n_\alpha, m_\alpha)$.

By using this transformation, the energy with the first modification becomes

$$V = \frac{1}{2}\{\sum_{\mathbf{k}_1,\mathbf{k}_2} \lambda(\mathbf{k}_1) z_1 z_2 \delta(\mathbf{k}_1+\mathbf{k}_2-\tau_1) + \sum_{\mathbf{k}_1,\mathbf{k}_2,\mathbf{k}_3} \gamma(\mathbf{k}_1) z_1 z_2 z_3 \delta(\mathbf{k}_1+\mathbf{k}_2+\mathbf{k}_3-\tau_2) + \sum_{\mathbf{k}_1,\mathbf{k}_2,\mathbf{k}_3,\mathbf{k}_4} z_1 z_2 z_3 z_4 \delta(\mathbf{k}_1+\mathbf{k}_2+\mathbf{k}_3+\mathbf{k}_4-\tau_3)\}. \tag{4.4}$$

where the dispersion function $\lambda(\mathbf{k})$ is as before in (3.4) and $\gamma(\mathbf{k})$ is given by

$$\gamma(\mathbf{k}) = H + 2C[\cos\frac{2\pi}{N}n + \cos\frac{2\pi}{N}m + \cos\frac{2\pi}{N}(n+m)]. \tag{4.5}$$

Similarly, the energy with the second modification becomes

$$V = \frac{1}{2}\{\sum_{\mathbf{k}_1,\mathbf{k}_2} \lambda(\mathbf{k}_1) z_1 z_2 \delta(\mathbf{k}_1+\mathbf{k}_2-\tau_1) + \sum_{\mathbf{k}_1,\mathbf{k}_2,\mathbf{k}_3} \gamma(\mathbf{k}_1,\mathbf{k}_2) z_1 z_2 z_3 \delta(\mathbf{k}_1+\mathbf{k}_2+\mathbf{k}_3-\tau_2) + \sum_{\mathbf{k}_1,\mathbf{k}_2,\mathbf{k}_3,\mathbf{k}_4} z_1 z_2 z_3 z_4 \delta(\mathbf{k}_1+\mathbf{k}_2+\mathbf{k}_3+\mathbf{k}_4-\tau_3)\}. \tag{4.6}$$

where the coefficient function $\lambda(\mathbf{k})$ is as before and $\gamma(\mathbf{k}_1,\mathbf{k}_2)$ is given by

$$\gamma(\mathbf{k}_1,\mathbf{k}_2) = H + 2D[\cos\tfrac{2\pi}{N}(n_1-m_2) + \cos\tfrac{2\pi}{N}(m_1+n_2+m_2) + \cos\tfrac{2\pi}{N}(n_1+m_1+n_2)]. \tag{4.7}$$

Notice how similar each of these is to the original transformed energy in (3.3). Because of this similarity, we show in Theorem 4.3 below that these modifications do nothing to alter the incorrect $\beta \to 3q\ inc \to 1q\ inc \to \alpha$ sequence of transitions.

## 4.2 Modifications to the quartic term

Just as there are many possible modifications to the cubic term in Parlinski's model, there are also several possibilities for additions to the quartic term. I list here three different terms

that could be added to the quartic term, each with a new parameter.

$$Ex_{j,l}^3(x_{j+1,l}+x_{j-1,l}+x_{j,l+1}+x_{j,l-1}+x_{j+1,l+1}+x_{j-1,l-1}) \tag{4.8}$$

$$Fx_{j,l}^2(x_{j+1,l}^2+x_{j-1,l}^2+x_{j,l+1}^2+x_{j,l-1}^2+x_{j+1,l+1}^2+x_{j-1,l-1}^2) \tag{4.9}$$

$$\begin{aligned} Gx_{j,l}^2(&x_{j+1,l}x_{j,l-1}+x_{j,l-1}x_{j-1,l-1}+x_{j-1,l-1}x_{j-1,l}+x_{j-1,l}x_{j,l+1} \\ &+x_{j,l+1}x_{j+1,l+1}+x_{j+1,l+1}x_{j+1,l}) \end{aligned} \tag{4.10}$$

Each of these involves nearest neighbor interactions only. Clearly creativity and an abundance of time could yield plenty of other interesting additions to the energy involving other neighbors, as shown in the following examples:

$$x_{j,l}^2(x_{j+1,l+1}x_{j-1,l-1}+x_{j+1,l}x_{j-1,l}+x_{j,l+1}x_{j,l-1}) \tag{4.11}$$

$$x_{j,l}(x_{j+1,l+1}x_{j-1,l}x_{j,l-1}+x_{j-1,l-1}x_{j+1,l}x_{j,l+1}). \tag{4.12}$$

In (4.11), the quartic interaction involves the center atom and the pair of its nearest neighbors which are at 180° to each other. These two are next-nearest neighbors to each other. In (4.12), the quartic interaction involves the center atom and its three nearest neighbors which are located at 120° to each other. Although this is not really a complicated term and may seem like a reasonable modification, these three atoms are not even next-nearest neighbors to each other. We will see, however, that each of these (along with all possible quartic modifications) reduces to the same case.

## 4.3 Why 2-D modifications will not work

All of the possible modifications listed above have in common the fact that they have hexagonal symmetry. Because of this, each of these reduces to a slight variation of Parlinski's original model. Including all of the possible nearest neighbor interactions in the cubic and quartic terms along with Parlinski's energy function, we get the general form of the energy

$$\begin{aligned} V=&\tfrac{1}{2}\textstyle\sum_{j,l}\{Ax_{j,l}^2+Bx_{j,l}(x_{j+1,l}+x_{j-1,l}+x_{j,l+1}+x_{j,l-1}+x_{j+1,l+1}+x_{j-1,l-1}) \\ &+x_{j,l}(x_{j+1,l-1}+x_{j-1,l+1}+x_{j+2,l+1}+x_{j-2,l-1}+x_{j+1,l+2}+x_{j-1,l-2}) \\ &+Hx_{j,l}^3+Cx_{j,l}^2(x_{j+1,l}+x_{j-1,l}+x_{j,l+1}+x_{j,l-1}+x_{j+1,l+1}+x_{j-1,l-1}) \\ &+Dx_{j,l}(x_{j+1,l}x_{j,l-1}+x_{j,l-1}x_{j-1,l-1}+x_{j-1,l-1}x_{j-1,l}+x_{j-1,l}x_{j,l+1}+x_{j,l+1}x_{j+1,l+1}+x_{j+1,l+1}x_{j+1,l}) \\ &+x_{j,l}^4+Ex_{j,l}^3(x_{j+1,l}+x_{j-1,l}+x_{j,l+1}+x_{j,l-1}+x_{j+1,l+1}+x_{j-1,l-1}) \\ &+Fx_{j,l}^2(x_{j+1,l}^2+x_{j-1,l}^2+x_{j,l+1}^2+x_{j,l-1}^2+x_{j+1,l+1}^2+x_{j-1,l-1}^2) \\ &+Gx_{j,l}^2(x_{j+1,l}x_{j,l-1}+x_{j,l-1}x_{j-1,l-1}+x_{j-1,l-1}x_{j-1,l}+x_{j-1,l}x_{j,l+1}+x_{j,l+1}x_{j+1,l+1}+x_{j+1,l+1}x_{j+1,l})\}. \end{aligned} \tag{4.13}$$

**Lemma 4.1.** *Using the discrete Fourier transformation, we get the following reductions into reciprocal space:*

$$\begin{aligned}
\sum_{j,l} x_{j,l}x_{j+p,l+r} &= \sum_{\mathbf{k}_1,\mathbf{k}_2} z_{\mathbf{k}_1}z_{\mathbf{k}_2}\delta(\mathbf{k}_1+\mathbf{k}_2-\tau_1)e^{-\frac{2\pi i}{N}(n_1p+m_1r)} \\
\sum_{j,l} x_{j,l}x_{j+p,l+r}x_{j+s,l+t} &= \sum_{\mathbf{k}_1,\mathbf{k}_2,\mathbf{k}_3} z_{\mathbf{k}_1}z_{\mathbf{k}_2}z_{\mathbf{k}_3}\delta(\mathbf{k}_1+\mathbf{k}_2+\mathbf{k}_3-\tau_2)e^{-\frac{2\pi i}{N}(n_1p+n_2s+m_1r+m_2t)} \\
\sum_{j,l} x_{j,l}x_{j+p,l+r}x_{j+s,l+t}x_{j+u,l+v} &= \sum_{\mathbf{k}_1,\mathbf{k}_2,\mathbf{k}_3,\mathbf{k}_4} z_{\mathbf{k}_1}z_{\mathbf{k}_2}z_{\mathbf{k}_3}z_{\mathbf{k}_4}\delta(\mathbf{k}_1+\mathbf{k}_2+\mathbf{k}_3+\mathbf{k}_4-\tau_3) \\
&\qquad e^{-\frac{2\pi i}{N}(n_1p+n_2s+n_3u+m_1r+m_2t+m_3v)}
\end{aligned}$$

*where $\tau_1$, $\tau_2$, and $\tau_3$ are vectors in the reciprical space, i.e. they have the form $\frac{2\pi n}{N}\mathbf{a}^*+\frac{2\pi m}{N}\mathbf{b}^*$ where $n$ and $m$ are integers. Here, we are centered on the atom at position $\mathbf{R}_{j,l}$ and its neighbors. These equations are true for any integers $p$, $r$, $s$, $t$, $u$, and $v$.*

*Proof.* There should be an $N^2$ in front of all of the summations, which I leave off for the sake of simplicity. As in Chapter 3, we will use the shorthand $W = e^{-\frac{2\pi i}{N}}$. Using the fact that

$$x_{j,l} = \sum_{\mathbf{k}} z_{\mathbf{k}}e^{(-i\mathbf{k}\cdot\mathbf{R}_{j,l})} = \sum_{\mathbf{k}} z_{\mathbf{k}}W^{nj}W^{ml},$$

we can multiply the displacement of two atoms together, as in the quadratic terms, to get

$$\begin{aligned}
x_{j,l}x_{j+p,l+r} &= \sum_{\mathbf{k}_1,\mathbf{k}_2} z_{\mathbf{k}_1}z_{\mathbf{k}_2}W^{n_1(j+p)}W^{m_1(l+r)}W^{n_2j}W^{m_2l} \\
&= \sum_{\mathbf{k}_1,\mathbf{k}_2} z_{\mathbf{k}_1}z_{\mathbf{k}_2}W^{n_1p}W^{m_1r}W^{(n_1+n_2)j}W^{(m_1+m_2)l}.
\end{aligned}$$

Now taking the summation over all $j$ and $l$, we have that

$$\begin{aligned}
\sum_{j,l} x_{j,l}x_{j+p,l+r} &= \sum_{\mathbf{k}_1,\mathbf{k}_2} z_{\mathbf{k}_1}z_{\mathbf{k}_2}W^{n_1p}W^{m_1r}\sum_j W^{(n_1+n_2)j}\sum_l W^{(m_1+m_2)l} \\
&= \sum_{\mathbf{k}_1,\mathbf{k}_2} z_{\mathbf{k}_1}z_{\mathbf{k}_2}W^{n_1p}W^{m_1r}\delta(\tfrac{n_1+n_2}{N}-\alpha_1)\delta(\tfrac{m_1+m_2}{N}-\alpha_2) \\
&= \sum_{\mathbf{k}_1,\mathbf{k}_2} z_{\mathbf{k}_1}z_{\mathbf{k}_2}W^{n_1p}W^{m_1r}\delta(\mathbf{k}_1+\mathbf{k}_2-\tau_1)
\end{aligned}$$

using the result from Lemma 3.1 and letting $\tau_1$ represent the reciprocal lattice vector $\frac{2\pi\alpha_1}{N}\mathbf{a}^*+\frac{2\pi\alpha_2}{N}\mathbf{b}^*$. This is the desired result for the quadratic terms.

Now for the cubic terms, we have

$$\begin{aligned}
x_{j,l}x_{j+p,l+r}x_{j+s,l+t} &= \sum_{\mathbf{k}_1,\mathbf{k}_2,\mathbf{k}_3} z_{\mathbf{k}_1}z_{\mathbf{k}_2}z_{\mathbf{k}_3}W^{n_1(j+p)}W^{m_1(l+r)}W^{n_2(j+s)}W^{m_2(l+t)}W^{n_3j}W^{m_3l} \\
&= \sum_{\mathbf{k}_1,\mathbf{k}_2,\mathbf{k}_3} z_{\mathbf{k}_1}z_{\mathbf{k}_2}z_{\mathbf{k}_3}W^{n_1p}W^{m_1r}W^{n_2s}W^{m_2t}W^{(n_1+n_2+n_3)j}W^{(m_1+m_2+m_3)l},
\end{aligned}$$

and the summation yields

$$\begin{aligned}\sum_{j,l} x_{j,l}x_{j+p,l+r} &= \sum_{\mathbf{k}_1,\mathbf{k}_2,\mathbf{k}_3} z_{\mathbf{k}_1} z_{\mathbf{k}_2} z_{\mathbf{k}_3} W^{n_1 p} W^{m_1 r} W^{n_2 s} W^{m_2 t} \sum_j W^{(n_1+n_2+n_3)j} \sum_l W^{(m_1+m_2+m_3)l} \\ &= \sum_{\mathbf{k}_1,\mathbf{k}_2,\mathbf{k}_3} z_{\mathbf{k}_1} z_{\mathbf{k}_2} z_{\mathbf{k}_3} W^{n_1 p} W^{m_1 r} W^{n_2 s} W^{m_2 t} \delta(\tfrac{n_1+n_2+n_3}{N} - \alpha_3)\delta(\tfrac{m_1+m_2+m_3}{N} - \alpha_4) \\ &= \sum_{\mathbf{k}_1,\mathbf{k}_2,\mathbf{k}_3} z_{\mathbf{k}_1} z_{\mathbf{k}_2} z_{\mathbf{k}_3} W^{n_1 p} W^{m_1 r} W^{n_2 s} W^{m_2 t} \delta(\mathbf{k}_1 + \mathbf{k}_2 + \mathbf{k}_3 - \tau_2)\end{aligned}$$

where $\tau_2 = \frac{2\pi\alpha_3}{N}\mathbf{a}^* + \frac{2\pi\alpha_4}{N}\mathbf{b}^*$.

Finally, the quartic terms act similarly. Multiplying four terms together gives us

$$\begin{aligned}x_{j,l}x_{j+p,l+r}x_{j+s,l+t}x_{j+u,l+v} &= \sum z_{\mathbf{k}_1} z_{\mathbf{k}_2} z_{\mathbf{k}_3} z_{\mathbf{k}_4} W^{n_1(j+p)} W^{m_1(l+r)} W^{n_2(j+s)} W^{m_2(l+t)} W^{n_3(j+u)} W^{m_3(l+v)} W^{n_4 j} W^{m_4 l} \\ &= \sum z_{\mathbf{k}_1} z_{\mathbf{k}_2} z_{\mathbf{k}_3} z_{\mathbf{k}_4} W^{n_1 p + n_2 s + n_3 u + m_1 r + m_2 t + m_3 v} W^{(n_1+n_2+n_3+n_4)j} W^{(m_1+m_2+m_3+m_4)l},\end{aligned}$$

and summing over $j$ and $l$ yields

$$\begin{aligned}&\textstyle\sum_{j,l} x_{j,l}x_{j+p,l+r}x_{j+s,l+t}x_{j+u,l+v} \\ &\quad = \sum z_{\mathbf{k}_1} z_{\mathbf{k}_2} z_{\mathbf{k}_3} z_{\mathbf{k}_4} W^{n_1 p + n_2 s + n_3 u + m_1 r + m_2 t + m_3 v} \textstyle\sum_j W^{(n_1+n_2+n_3+n_4)j} \sum_l W^{(m_1+m_2+m_3+m_4)l} \\ &\quad = \sum z_{\mathbf{k}_1} z_{\mathbf{k}_2} z_{\mathbf{k}_3} z_{\mathbf{k}_4} W^{n_1 p + n_2 s + n_3 u + m_1 r + m_2 t + m_3 v} \delta(\tfrac{n_1+n_2+n_3+n_4}{N} - \alpha_5)\delta(\tfrac{m_1+m_2+m_3+m_4}{N} - \alpha_6) \\ &\quad = \sum z_{\mathbf{k}_1} z_{\mathbf{k}_2} z_{\mathbf{k}_3} z_{\mathbf{k}_4} W^{n_1 p + n_2 s + n_3 u + m_1 r + m_2 t + m_3 v} \delta(\mathbf{k}_1 + \mathbf{k}_2 + \mathbf{k}_3 + \mathbf{k}_4 - \tau_3)\end{aligned}$$

where $\tau_3 = \frac{2\pi\alpha_5}{N}\mathbf{a}^* + \frac{2\pi\alpha_6}{N}\mathbf{b}^*$ and the summations are on the vectors $\mathbf{k}_1$, $\mathbf{k}_2$, $\mathbf{k}_3$, and $\mathbf{k}_4$. □

As we will see in the following theorem, we can use this lemma many times to reduce the energy to

$$\begin{aligned}V = \frac{1}{2}\{ &\sum_{\mathbf{k}_1,\mathbf{k}_2} \lambda(\mathbf{k}_1) z_{\mathbf{k}_1} z_{\mathbf{k}_2} \delta(\mathbf{k}_1 + \mathbf{k}_2 - \tau_1) + \sum_{\mathbf{k}_1,\mathbf{k}_2,\mathbf{k}_3} \gamma(\mathbf{k}_1, \mathbf{k}_2) z_{\mathbf{k}_1} z_{\mathbf{k}_2} z_{\mathbf{k}_3} \delta(\mathbf{k}_1 + \mathbf{k}_2 + \mathbf{k}_3 - \tau_2) \\ &+ \sum_{\mathbf{k}_1,\mathbf{k}_2,\mathbf{k}_3,\mathbf{k}_4} \eta(\mathbf{k}_1, \mathbf{k}_2, \mathbf{k}_3) z_{\mathbf{k}_1} z_{\mathbf{k}_2} z_{\mathbf{k}_3} z_{\mathbf{k}_4} \delta(\mathbf{k}_1 + \mathbf{k}_2 + \mathbf{k}_3 + \mathbf{k}_4 - \tau_3)\}\end{aligned} \tag{4.14}$$

using this transformation.

**Theorem 4.2.** *The most general energy function (4.13), with hexagonal symmetry involving nearest and next-nearest neighbor interactions in the quadratic term and nearest neighbor interactions in the cubic and quartic terms, will reduce to (4.14) where $\lambda$, $\gamma$, and $\eta$ are as follows:*

$$\begin{aligned}\lambda(\mathbf{k}_1) =& A + 2B[\cos\tfrac{2\pi}{N}n_1 + \cos\tfrac{2\pi}{N}m_1 + \cos\tfrac{2\pi}{N}(n_1+m_1)] \\ &+ 2[\cos\tfrac{2\pi}{N}(n_1-m_1) + \cos\tfrac{2\pi}{N}(2n_1+m_1) + \cos\tfrac{2\pi}{N}(n_1+2m_1)] \\ \gamma(\mathbf{k}_1,\mathbf{k}_2) =& H + 2C[\cos\tfrac{2\pi}{N}n_1 + \cos\tfrac{2\pi}{N}m_1 + \cos\tfrac{2\pi}{N}(n_1+m_1)] \\ &+ 2D[\cos\tfrac{2\pi}{N}(n_1-m_2) + \cos\tfrac{2\pi}{N}(m_1+n_2+m_2) + \cos\tfrac{2\pi}{N}(n_1+m_1+n_2)] \\ \eta(\mathbf{k}_1,\mathbf{k}_2) =& 1 + 2E[\cos\tfrac{2\pi}{N}n_1 + \cos\tfrac{2\pi}{N}m_1 + \cos\tfrac{2\pi}{N}(n_1+m_1)] \\ &+ 2F[\cos\tfrac{2\pi}{N}(n_1+n_2) + \cos\tfrac{2\pi}{N}(m_1+m_2) + \cos\tfrac{2\pi}{N}(n_1+m_1+n_2+m_2)] \\ &+ 2G[\cos\tfrac{2\pi}{N}(n_1-m_2) + \cos\tfrac{2\pi}{N}(m_1+n_2+m_2) + \cos\tfrac{2\pi}{N}(n_1+m_1+n_2)]\end{aligned}$$

*Here we have written the wave vectors* $\mathbf{k}_j$ *as* $\frac{2\pi n_j}{N}\mathbf{a}^* + \frac{2\pi m_j}{N}\mathbf{b}^*$.

*Proof.* The quadratic part of the energy (4.13) is identical to that in Parlinski's original model. We have shown that the coefficient of the quadratic term is that listed above in the derivation of (3.4).

For the remaining terms, we will list them individually. In each case, we apply the appropriate identity from Lemma 4.1 to get the part of the coefficient from that term. The cubic terms are as follows:

$$\sum_{j,l} x_{j,l}^3 = N^2 \sum_{\mathbf{k}_1,\mathbf{k}_2,\mathbf{k}_3} z_{\mathbf{k}_1} z_{\mathbf{k}_2} z_{\mathbf{k}_3} \delta(\mathbf{k}_1+\mathbf{k}_2+\mathbf{k}_3-\tau_2)$$

$$\sum_{j,l} x_{j,l}^2 (x_{j+1,l}+x_{j-1,l}+x_{j,l+1}+x_{j,l-1}+x_{j+1,l+1}+x_{j-1,l-1})$$

$$= N^2 \sum_{\mathbf{k}_1,\mathbf{k}_2,\mathbf{k}_3} z_{\mathbf{k}_1} z_{\mathbf{k}_2} z_{\mathbf{k}_3} \delta(\mathbf{k}_1+\mathbf{k}_2+\mathbf{k}_3-\tau_2)[e^{-\frac{2\pi i}{N}n_1} + e^{\frac{2\pi i}{N}n_1} + e^{-\frac{2\pi i}{N}m_1} + e^{\frac{2\pi i}{N}m_1} + e^{-\frac{2\pi i}{N}(n_1+m_1)} + e^{\frac{2\pi i}{N}(n_1+m_1)}]$$

$$= N^2 \sum_{\mathbf{k}_1,\mathbf{k}_2,\mathbf{k}_3} z_{\mathbf{k}_1} z_{\mathbf{k}_2} z_{\mathbf{k}_3} \delta(\mathbf{k}_1+\mathbf{k}_2+\mathbf{k}_3-\tau_2) 2[\cos\tfrac{2\pi}{N}n_1 + \cos\tfrac{2\pi}{N}m_1 + \cos\tfrac{2\pi}{N}(n_1+m_1)]$$

$$\sum_{j,l} x_{j,l}(x_{j+1,l}x_{j,l-1} + x_{j,l-1}x_{j-1,l-1} + x_{j-1,l-1}x_{j-1,l} + x_{j-1,l}x_{j,l+1} + x_{j,l+1}x_{j+1,l+1} + x_{j+1,l+1}x_{j+1,l})$$

$$= N^2 \sum_{\mathbf{k}_1,\mathbf{k}_2,\mathbf{k}_3} z_{\mathbf{k}_1} z_{\mathbf{k}_2} z_{\mathbf{k}_3} \delta(\mathbf{k}_1+\mathbf{k}_2+\mathbf{k}_3-\tau_2)$$
$$[e^{-\frac{2\pi i}{N}(n_1-m_2)} + e^{\frac{2\pi i}{N}(m_1+n_2+m_2)} + e^{\frac{2\pi i}{N}(n_1+m_1+n_2)} + e^{\frac{2\pi i}{N}(n_1-m_2)} + e^{-\frac{2\pi i}{N}(m_1+n_2+m_2)} + e^{-\frac{2\pi i}{N}(n_1+m_1+n_2)}]$$

$$= N^2 \sum_{\mathbf{k}_1,\mathbf{k}_2,\mathbf{k}_3} z_{\mathbf{k}_1} z_{\mathbf{k}_2} z_{\mathbf{k}_3} \delta(\mathbf{k}_1+\mathbf{k}_2+\mathbf{k}_3-\tau_2)[\cos\tfrac{2\pi}{N}(n_1-m_2) + \cos\tfrac{2\pi}{N}(m_1+n_2+m_2) + \cos\tfrac{2\pi}{N}(n_1+m_1+n_2)].$$

Summing these terms with the appropriate parameters gives the coefficient function $\gamma(\mathbf{k}_1, \mathbf{k}_2)$.

The quartic terms reduce as follows:

$$\sum_{j,l} x_{j,l}{}^4 = N^2 \sum_{\mathbf{k}_1,\mathbf{k}_2,\mathbf{k}_3,\mathbf{k}_4} z_{\mathbf{k}_1} z_{\mathbf{k}_2} z_{\mathbf{k}_3} z_{\mathbf{k}_4} \delta(\mathbf{k}_1+\mathbf{k}_2+\mathbf{k}_3+\mathbf{k}_4-\tau_3)$$

$$\sum_{j,l} x_{j,l}{}^3 (x_{j+1,l}+x_{j-1,l}+x_{j,l+1}+x_{j,l-1}+x_{j+1,l+1}+x_{j-1,l-1})$$

$$= N^2 \sum_{\mathbf{k}_1,\mathbf{k}_2,\mathbf{k}_3,\mathbf{k}_4} z_{\mathbf{k}_1} z_{\mathbf{k}_2} z_{\mathbf{k}_3} z_{\mathbf{k}_4} \delta(\mathbf{k}_1+\mathbf{k}_2+\mathbf{k}_3-\tau_2)[e^{-\frac{2\pi i}{N}n_1} + e^{\frac{2\pi i}{N}n_1}$$
$$+ e^{-\frac{2\pi i}{N}m_1} + e^{\frac{2\pi i}{N}m_1} + e^{-\frac{2\pi i}{N}(n_1+m_1)} + e^{\frac{2\pi i}{N}(n_1+m_1)}]$$

$$= N^2 \sum_{\mathbf{k}_1,\mathbf{k}_2,\mathbf{k}_3,\mathbf{k}_4} z_{\mathbf{k}_1} z_{\mathbf{k}_2} z_{\mathbf{k}_3} z_{\mathbf{k}_4} \delta(\mathbf{k}_1+\mathbf{k}_2+\mathbf{k}_3-\tau_2) 2[\cos\tfrac{2\pi}{N}n_1 + \cos\tfrac{2\pi}{N}m_1 + \cos\tfrac{2\pi}{N}(n_1+m_1)]$$

$$\sum_{j,l} x_{j,l}{}^2 (x_{j+1,l}^2 + x_{j-1,l}^2 + x_{j,l+1}^2 + x_{j,l-1}^2 + x_{j+1,l+1}^2 + x_{j-1,l-1}^2)$$

$$= N^2 \sum_{\mathbf{k}_1,\mathbf{k}_2,\mathbf{k}_3,\mathbf{k}_4} z_{\mathbf{k}_1} z_{\mathbf{k}_2} z_{\mathbf{k}_3} z_{\mathbf{k}_4} \delta(\mathbf{k}_1+\mathbf{k}_2+\mathbf{k}_3-\tau_2)[e^{-\frac{2\pi i}{N}(n_1+n_2)} + e^{\frac{2\pi i}{N}(n_1+n_2)}$$
$$+ e^{-\frac{2\pi i}{N}(m_1+m_2)} + e^{\frac{2\pi i}{N}(m_1+m_2)} + e^{-\frac{2\pi i}{N}(n_1+n_2+m_1+m_2)} + e^{\frac{2\pi i}{N}(n_1+n_2+m_1+m_2)}]$$

$$= N^2 \sum_{\mathbf{k}_1,\mathbf{k}_2,\mathbf{k}_3,\mathbf{k}_4} z_{\mathbf{k}_1} z_{\mathbf{k}_2} z_{\mathbf{k}_3} z_{\mathbf{k}_4} \delta(\mathbf{k}_1+\mathbf{k}_2+\mathbf{k}_3-\tau_2) 2[\cos\tfrac{2\pi}{N}(n_1+n_2) + \cos\tfrac{2\pi}{N}(m_1+m_2) + \cos\tfrac{2\pi}{N}(n_1+n_2+m_1+m_2)]$$

$$\sum_{j,l} x_{j,l}{}^2 (x_{j+1,l}x_{j,l-1} + x_{j,l-1}x_{j-1,l-1} + x_{j-1,l-1}x_{j-1,l} + x_{j-1,l}x_{j,l+1} + x_{j,l+1}x_{j+1,l+1} + x_{j+1,l+1}x_{j+1,l})\}$$

$$= N^2 \sum_{\mathbf{k}_1,\mathbf{k}_2,\mathbf{k}_3,\mathbf{k}_4} z_{\mathbf{k}_1} z_{\mathbf{k}_2} z_{\mathbf{k}_3} z_{\mathbf{k}_4} \delta(\mathbf{k}_1+\mathbf{k}_2+\mathbf{k}_3-\tau_2)[e^{-\frac{2\pi i}{N}(n_1-m_2)} + e^{\frac{2\pi i}{N}(-m_1-n_2-m_2)}$$
$$+ e^{-\frac{2\pi i}{N}(-n_1-m_1-n_2)} + e^{\frac{2\pi i}{N}(-n_1+m_2)} + e^{-\frac{2\pi i}{N}(m_1+n_2+m_2)} + e^{\frac{2\pi i}{N}(n_1+m_1+n2)}]$$

$$= N^2 \sum_{\mathbf{k}_1,\mathbf{k}_2,\mathbf{k}_3,\mathbf{k}_4} z_{\mathbf{k}_1} z_{\mathbf{k}_2} z_{\mathbf{k}_3} z_{\mathbf{k}_4} \delta(\mathbf{k}_1+\mathbf{k}_2+\mathbf{k}_3-\tau_2) 2[\cos\tfrac{2\pi}{N}(n_1-m_2) + \cos\tfrac{2\pi}{N}(m_1+n_2+m_2) + \cos\tfrac{2\pi}{N}(n_1+m_1+n_2)]$$

By multiplying by the parameters given in (4.13) and adding each of these, we get the coefficient function $\eta(\mathbf{k}_1, \mathbf{k}_2)$. □

**Theorem 4.3.** *Any energy function with hexagonal symmetry which involves interactions of any number of neighbors will reduce to (4.14) in reciprocal space.*

*Proof.* In order for a model to have hexagonal symmetry and involve interactions of neighbors, it is necessary for us to understand what terms must be included to achieve that symmetry. We have seen examples of such interactions from Parlinski's model and the modifications that we have proposed. We would like, however, to be able to write a general term with hexagonal symmetry which may represent any neighbor. To do this, we turn to the general quadratic, cubic, and quartic terms in Lemma 4.1 and focus on the symmetry in the hexagonal lattice.

By looking at the lattice, we can see which terms that $x_{j+p,l+r}$ would be mapped into by successive rotations of 60° around $x_{j,l}$. Doing this, we see that $x_{j+p,l+r}$ is rotationally equivalent to $x_{j-p+r,l-p}$, $x_{j-r,l+p-r}$, $x_{j-p,l-r}$, $x_{j+p-r,l+p}$, and $x_{j+r,l-p+r}$. So if the quadratic part of the energy is to include a term of $x_{j,l}x_{j+p,l+r}$, then it must include all six of the terms

$$x_{j,l}(x_{j+p,l+r} + x_{j-p+r,l-p} + x_{j-r,l+p-r} + x_{j-p,l-r} + x_{j+p-r,l+p} + x_{j+r,l-p+r}).$$

We can see that this term can describe both the nearest neighbor and next-nearest neighbor terms by appropriate choices of $p$ and $r$.

Using the results of Lemma 4.1, summing this general quadratic term over $j$ and $l$ reduces to

$$\begin{aligned}
&\sum_{j,l} x_{j,l}(x_{j+p,l+r} + x_{j-p+r,l-p} + x_{j-r,l+p-r} + x_{j-p,l-r} + x_{j+p-r,l+p} + x_{j+r,l-p+r}) \\
&\quad = \sum_{\mathbf{k}_1,\mathbf{k}_2} z_{\mathbf{k}_1} z_{\mathbf{k}_2} \delta(\mathbf{k}_1 + \mathbf{k}_2 - \tau_1)[e^{-\frac{2\pi i}{N}(n_1 p + m_1 r)} + e^{-\frac{2\pi i}{N}(n_1(-p+r)+m_1(-p))} + e^{-\frac{2\pi i}{N}(n_1(-r)+m_1(p-r))} \\
&\qquad\qquad + e^{\frac{2\pi i}{N}(n_1 p + m_1 r)} + e^{\frac{2\pi i}{N}(n_1(-p+r)+m_1(-p))} + e^{\frac{2\pi i}{N}(n_1(-r)+m_1(p-r))}] \\
&\quad = \sum_{\mathbf{k}_1,\mathbf{k}_2} z_{\mathbf{k}_1} z_{\mathbf{k}_2} \delta(\mathbf{k}_1 + \mathbf{k}_2 - \tau_1) 2[\cos\tfrac{2\pi}{N}(n_1 p + m_1 r) \\
&\qquad\qquad + \cos\tfrac{2\pi}{N}(n_1(p-r) + m_1 p) + \cos\tfrac{2\pi}{N}(n_1 r + m_1(-p+r))]
\end{aligned}$$

Thus any quadratic interaction which maintains the hexagonal symmetry can be transformed into reciprocal space using this reduction. This means that the coefficient of the quadratic term would include

$$2[\cos\tfrac{2\pi}{N}(n_1 p + m_1 r) + \cos\tfrac{2\pi}{N}(n_1(p-r) + m_1 p) + \cos\tfrac{2\pi}{N}(n_1 r + m_1(-p+r))].$$

This term maintains the hexagonal symmetry, so even if there are several different quadratic terms involving different distance neighbors, they each have a coefficient of this form when transformed into reciprocal space. The sum of the coefficients of these terms will be $\lambda(\mathbf{k}_1)$ in (4.14).

The cubic terms work similarly, but they are more complicated to look at because there can be up to three different atoms that are interacting. If we include the term $x_{j,l}x_{j+p,l+r}x_{j+s,l+t}$, then the symmetry requires that we include all of the terms

$$\begin{aligned}
x_{j,l}(&x_{j+p,l+r}x_{j+s,l+t} + x_{j-p+r,l-p}x_{j-s+t,l-s} + x_{j-r,l+p-r}x_{j-t,l+s-t} \\
&+ x_{j-p,l-r}x_{j-s,l-t} + x_{j+p-r,l+p}x_{j+s-t,l+s} + x_{j+r,l-p+r}x_{j+t,l-s+t}).
\end{aligned}$$

Summing these over $j$ and $l$ gives us

$$\begin{aligned}
&\sum_{j,l} x_{j,l}(x_{j+p,l+r}x_{j+s,l+t} + x_{j-p+r,l-p}x_{j-s+t,l-s} + x_{j-r,l+p-r}x_{j-t,l+s-t} \\
&\qquad + x_{j-p,l-r}x_{j-s,l-t} + x_{j+p-r,l+p}x_{j+s-t,l+s} + x_{j+r,l-p+r}x_{j+t,l-s+t}) \\
&= \sum_{\mathbf{k}_1,\mathbf{k}_2,\mathbf{k}_3} z_{\mathbf{k}_1}z_{\mathbf{k}_2}z_{\mathbf{k}_3}\delta(\mathbf{k}_1+\mathbf{k}_2+\mathbf{k}_3-\tau_2)[e^{-\frac{2\pi i}{N}(n_1p+n_2s+m_1r+m_2t)} \\
&\qquad + e^{-\frac{2\pi i}{N}(n_1(-p+r)+n_2(-s+t)+m_1(-p)+m_2(-s))} \\
&\qquad + e^{-\frac{2\pi i}{N}(n_1(-r)+n_2(-t)+m_1(p-r)+m_2(s-t))} + e^{\frac{2\pi i}{N}(n_1p+n_2s+m_1r+m_2t)} \\
&\qquad + e^{\frac{2\pi i}{N}(n_1(-p+r)+n_2(-s+t)+m_1(-p)+m_2(-s))} + e^{\frac{2\pi i}{N}(n_1(-r)+n_2(-t)+m_1(p-r)+m_2(s-t))}] \\
&= \sum_{\mathbf{k}_1,\mathbf{k}_2,\mathbf{k}_3} z_{\mathbf{k}_1}z_{\mathbf{k}_2}z_{\mathbf{k}_3}\delta(\mathbf{k}_1+\mathbf{k}_2+\mathbf{k}_3-\tau_2)2[\cos\tfrac{2\pi}{N}(n_1p+n_2s+m_1r+m_2t) \\
&\qquad + \cos\tfrac{2\pi}{N}(n_1(p-r)+n_2(s-t)+m_1p+m_2s) \\
&\qquad + \cos\tfrac{2\pi}{N}(n_1r+n_2t+m_1(-p+r)+m_2(-s+t))]
\end{aligned} \tag{4.15}$$

Therefore, the coefficient of the cubic term, $\gamma(\mathbf{k}_1,\mathbf{k}_2)$, will be a (summation of) term(s) of the form

$$\begin{aligned}
&2[\cos\tfrac{2\pi}{N}(n_1p+n_2s+m_1r+m_2t) + \cos\tfrac{2\pi}{N}(n_1(p-r)+n_2(s-t)+m_1p+m_2s) \\
&\qquad + \cos\tfrac{2\pi}{N}(n_1r+n_2t+m_1(-p+r)+m_2(-s+t))].
\end{aligned}$$

Since this has hexagonal symmetry, then $\gamma(\mathbf{k}_1,\mathbf{k}_2)$ will have hexagonal symmetry also.

For the quartic terms, we can have $x_{j,l}x_{j+p,l+r}x_{j+s,l+t}x_{j+u,l+v}$. If we have this term, then the symmetry requires that we have the six terms

$$\begin{aligned}
&x_{j,l}(x_{j+p,l+r}x_{j+s,l+t}x_{j+u,l+v} + x_{j-p+r,l-p}x_{j-s+t,l-s}x_{j-u+v,l-u} \\
&\quad + x_{j-r,l+p-r}x_{j-t,l+s-t}x_{j-v,l+u-v} + x_{j-p,l-r}x_{j-s,l-t}x_{j-u,l-v} \\
&\quad + x_{j+p-r,l+p}x_{j+s-t,l+s}x_{j+u-v,l+u} + x_{j+r,l-p+r}x_{j+t,l-s+t}x_{j+v,l-u+v}).
\end{aligned}$$

Now taking the summation over all lattice points gives us

$$\begin{aligned}
&\sum_{j,l} x_{j,l}(x_{j+p,l+r}x_{j+s,l+t}x_{j+u,l+v} + x_{j-p+r,l-p}x_{j-s+t,l-s}x_{j-u+v,l-u} \\
&\qquad + x_{j-r,l+p-r}x_{j-t,l+s-t}x_{j-v,l+u-v} + x_{j-p,l-r}x_{j-s,l-t}x_{j-u,l-v} \\
&\qquad + x_{j+p-r,l+p}x_{j+s-t,l+s}x_{j+u-v,l+u} + x_{j+r,l-p+r}x_{j+t,l-s+t}x_{j+v,l-u+v}) \\
&= \sum_{\mathbf{k}_1,\mathbf{k}_2,\mathbf{k}_3,\mathbf{k}_4} z_{\mathbf{k}_1}z_{\mathbf{k}_2}z_{\mathbf{k}_3}z_{\mathbf{k}_4}\delta(\mathbf{k}_1+\mathbf{k}_2+\mathbf{k}_3+\mathbf{k}_4-\tau_3)[e^{-\frac{2\pi i}{N}(n_1p+n_2s+n_3u+m_1r+m_2t+m_3v)} \\
&\qquad + e^{-\frac{2\pi i}{N}(n_1(-p+r)+n_2(-s+t)+n_3(-u_v)+m_1(-p)+m_2(-s)+m_3(-u))} \\
&\qquad + e^{-\frac{2\pi i}{N}(n_1(-r)+n_2(-t)+n_3(-v)+m_1(p-r)+m_2(s-t)+m_3(u-v)} \\
&\qquad + e^{\frac{2\pi i}{N}(n_1p+n_2s+n_3u+m_1r+m_2t+m_3v)} \\
&\qquad + e^{\frac{2\pi i}{N}(n_1(-p+r)+n_2(-s+t)+n_3(-u_v)+m_1(-p)+m_2(-s)+m_3(-u))} \\
&\qquad + e^{\frac{2\pi i}{N}(n_1(-r)+n_2(-t)+n_3(-v)+m_1(p-r)+m_2(s-t)+m_3(u-v)}] \\
&= \sum_{\mathbf{k}_1,\mathbf{k}_2,\mathbf{k}_3,\mathbf{k}_4} z_{\mathbf{k}_1}z_{\mathbf{k}_2}z_{\mathbf{k}_3}z_{\mathbf{k}_4}\delta(\mathbf{k}_1+\mathbf{k}_2+\mathbf{k}_3+\mathbf{k}_4-\tau_3)\times \\
&\qquad 2[\cos\tfrac{2\pi}{N}(n_1p+n_2s+n_3u+m_1r+m_2t+m_3v) \\
&\qquad + \cos\tfrac{2\pi}{N}(n_1(p-r)+n_2(s-t)+n_3(u-v)+m_1p+m_2s+m_3u) \\
&\qquad + \cos\tfrac{2\pi}{N}(n_1r+n_2t+n_3v+m_1(-p+r)+m_2(-s+t)+m_3(-u+v))].
\end{aligned} \tag{4.16}$$

Hence $\eta$, the coefficient of the quadratic term of (4.14), would have terms of the form

$$\begin{aligned}
&2[\cos\tfrac{2\pi}{N}(n_1p+n_2s+n_3u+m_1r+m_2t+m_3v) \\
&\qquad + \cos\tfrac{2\pi}{N}(n_1(p-r)+n_2(s-t)+n_3(u-v)+m_1p+m_2s+m_3u) \\
&\qquad + \cos\tfrac{2\pi}{N}(n_1r+n_2t+n_3v+m_1(-p+r)+m_2(-s+t)+m_3(-u+v))].
\end{aligned}$$

□

**Theorem 4.4.** *Any energy function of the form (4.14) will have the bifurcation diagram shown in Figure 4.2. In particular, the hexagons always become stable before the rolls.*

*Proof.* With a function of the form (4.14), we can find approximate solutions by taking a first-order approximation. By doing this we can write the approximation of the energy as

$$\begin{aligned}
\tilde{V} =&\lambda(z_1^2+z_2^2+z_3^2) + 6\gamma z_1z_2z_3 + 3\eta(z_1^4+z_2^4+z_3^4) \\
&+ 12\eta(z_1^2z_2^2+z_1^2z_3^2+z_2^2z_3^2)\}.
\end{aligned} \tag{4.17}$$

where the $z_i$'s are the amplitudes of the normal modes and $\lambda$, $\gamma$, and $\eta$ are the values of those corresponding functions.

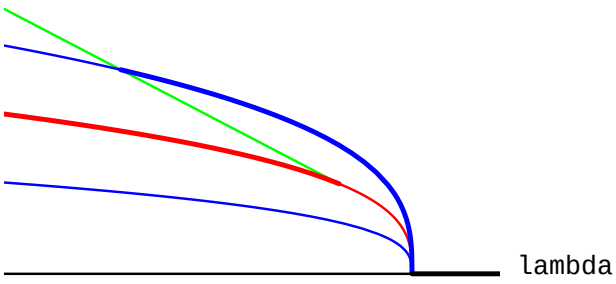


Figure 4.2: The bifurcation diagram of the general energy function. The red, green, and blue curves correspond to the $1q$, $2q$, and $3q$ solutions, respectively. Stable solutions are shown as thick curves while unstable solutions are thin. The horizontal axis represents the bifurcation parameter $\lambda$, while the vertical axis has no meaning; the curves are merely drawn to show the branches clearly.

Now $\nabla\tilde{V}$ is of the form

$$\nabla_z\tilde{V} = g(z) = \begin{pmatrix} 2\lambda z_1 + 6\gamma\bar{z}_2\bar{z}_3 + 12\eta z_1|z_1|^2 + 24\eta z_1(|z_2|^2 + |z_3|^2) \\ 2\lambda z_2 + 6\gamma\bar{z}_1\bar{z}_3 + 12\eta z_2|z_2|^2 + 24\eta z_2(|z_1|^2 + |z_3|^2) \\ 2\lambda z_3 + 6\gamma\bar{z}_1\bar{z}_2 + 12\eta z_3|z_3|^2 + 24\eta z_3(|z_2|^2 + |z_2|^2) \end{pmatrix}$$

We can rewrite this to match the notation of Golubitsky from the Chapter 2. For example, by writing the vector as

$$g(z) = \begin{pmatrix} z_1(2\lambda + 24\eta\sigma_1 - 12\eta|z_1|^2) + \bar{z}_2\bar{z}_3(6\gamma) \\ z_2(2\lambda + 24\eta\sigma_1 - 12\eta|z_2|^2) + \bar{z}_1\bar{z}_3(6\gamma) \\ z_3(2\lambda + 24\eta\sigma_1 - 12\eta|z_3|^2) + \bar{z}_1\bar{z}_2(6\gamma) \end{pmatrix},$$

we have $g(z)$ in the form (2.3) where $H_j = h_1 + u_j h_3 + u_j^2 h_5$ and $P_j = p_2 + u_j p_4 + u_j^2 p_6$. For Parlinski's model, $h_1 = 2\lambda + 24\eta\sigma_1$, $h_3 = -12\eta$, $h_5 = 0$, $p_2 = 6\gamma$, $p_4 = 0$, and $p_6 = 0$. Recall that $\sigma_1 = |z_1|^2 + |z_2|^2 + |z_3|^2$ and $u_j = |z_j|^2$. This falls into the case discussed in section 2.4, so we can apply those results directly. For the notation of that section, we have $a = 24\eta$, $b = -12\eta$, and $e = 6\gamma$.

The solutions to $g(z, \lambda) = 0$ are given in real coordinates by:

(II) Rolls: $x_1 = \sqrt{\frac{-\lambda}{6\eta}}$

(III) Hexagons: $x_1 = \frac{1}{60\eta}(-3\gamma \pm \sqrt{9\gamma^2 - 120\eta\lambda})$

(IV) Rectangles: $x_1 = \frac{-\gamma}{2\eta}$ and $x_2 = \sqrt{\frac{-2\eta\lambda - 3\gamma^2}{36\eta^2}}$.

From Table 2.4, it is easy to compute the eigenvalues for the different branches of solutions. They are listed in Table 4.3.

By looking at the sign of the eigenvalues, we can determine the stability of the different branches of solutions. Since the problem that we are solving is $\ddot{z} = -\nabla_z \tilde{V}$, the solutions will be stable where all of the eigenvalues are positive, and the solutions will be unstable where any eigenvalue is negative. For the zero eigenvalues, more work is required.

The trivial solution is clearly stable when $\lambda > 0$ and unstable when $\lambda < 0$.

The rolls only exist when $\lambda < 0$ because $x_1 = \sqrt{\frac{-\lambda}{6\eta}}$ is real. Thus the first eigenvalue, $-4\lambda$, is positive. The second and third eigenvalues are both positive if $-2\eta\lambda > \pm\gamma\sqrt{-6\lambda}$. Depending on the sign of $\gamma$, the inequality is trivial if $\pm\gamma < 0$. For $\pm\gamma > 0$, squaring both sides and dividing by $4\eta^2\lambda$ yields $\lambda < \frac{-3\gamma^2}{2\eta^3}$. This is the restriction on $\lambda$ for which the rolls will be stable, but we must study the zero eigenvalue in order to prove that.

In order for the hexagons to be real, we must have that $\lambda \leq \frac{3\gamma^2}{40\eta}$. If we only consider that $\lambda < 0$, then we have that $\sqrt{9\gamma^2 - 120\eta\lambda} > \sqrt{9\gamma^2} = 3\gamma\text{sgn}(\gamma)$. The two types of hexagons have opposite stability, depending on the sign of the parameter $\gamma$. Consider this for the third eigenvalue listed for the hexagon solutions:

$$\frac{3}{10}(3\gamma^2 - \gamma\text{sgn}(\gamma)\sqrt{9\gamma^2 - 120\eta\lambda}) < \frac{3}{10}(3\gamma^2 - \gamma\text{sgn}(\gamma)(3\gamma\text{sgn}(\gamma))) = 0.$$

This means that $\text{III}^+$ solutions will be unstable if $\gamma > 0$ and $\text{III}^-$ solutions will be unstable if $\gamma < 0$.

Setting the first eigenvalue equal to zero and simplifying the equation, we get

$$5\eta\lambda + 3\gamma^2 = \pm\gamma\sqrt{9\gamma^2 - 120\eta\lambda},$$

where $\gamma$ is positive for $\text{III}^-$ solutions and negative for $\text{III}^+$ solutions. Squaring both sides and solving for $\lambda$, we get that either $\lambda = 0$ or $\lambda = -6\frac{\gamma^2}{\eta}$. Thus the eigenvalue is positive if $-6\frac{\gamma^2}{\eta} < \lambda < 0$. The other eigenvalue is positive in this region also, so we need to study the zero eigenvalue to determine the actual region of stability.

The rectangles show no stable region. Since $x_2 = \pm\sqrt{\frac{-2\eta\lambda - 3\gamma^2}{36\eta^2}}$ is real, we must have that $\lambda < \frac{-3\gamma^2}{2\eta}$ for the solution to exist. The first eigenvalue for rectangles listed in Table 4.3 is $\frac{4}{3}\lambda + 8\frac{\gamma^2}{\eta}$. This must be greater than 0 in order for the solution to be stable, so this requires that $\lambda > -6\frac{\gamma^2}{\eta}$. Now consider the last eigenvalue for rectangles. If this eigenvalue is greater

Table 4.1: Eigenvalues for each type of solution in the modifications to Parlinski's model.

| | Nomenclature | Eigenvalue | Multiplicity |
|---|---|---|---|
| I | Trivial | $2\lambda$ | 6 |
| II | Rolls | $-4\lambda$ | 1 |
| | | $-2\eta\lambda - \gamma\sqrt{-\frac{6\lambda}{\eta}}$ | 2 |
| | | $-2\eta\lambda + \gamma\sqrt{-\frac{6\lambda}{\eta}}$ | 2 |
| | | $0$ | 1 |
| III$^+$ | Hexagons$^+$ | $\frac{4}{25\eta}(5\eta\lambda + 3\gamma^2 - \gamma\sqrt{9\gamma^2 - 120\eta\lambda})$ | 2 |
| | | $\frac{1}{10\eta}(-40\eta\lambda + 3\gamma^2 - \gamma\sqrt{9\gamma^2 - 120\eta\lambda})$ | 1 |
| | | $\frac{3}{10\eta}(3\gamma^2 - \gamma\sqrt{9\gamma^2 - 120\eta\lambda})$ | 1 |
| | | $0$ | 2 |
| III$^-$ | Hexagons$^-$ | $\frac{4}{25\eta}(5\eta\lambda + 3\gamma^2 + \gamma\sqrt{9\gamma^2 - 120\eta\lambda})$ | 2 |
| | | $\frac{1}{10\eta}(-40\eta\lambda + 3\gamma^2 + \gamma\sqrt{9\gamma^2 - 120\eta\lambda})$ | 1 |
| | | $\frac{3}{10\eta}(3\gamma^2 + \gamma\sqrt{9\gamma^2 - 120\eta\lambda})$ | 1 |
| | | $0$ | 2 |
| IV | Rectangles | $\frac{4}{3}\lambda + \frac{8\gamma^2}{\eta}$ | 1 |
| | | $-\frac{2}{3}\lambda + \frac{5\gamma^2}{\eta}$ | 1 |
| | | $0$ | 2 |
| | | $\frac{1}{6}(-14\lambda - 3\frac{\gamma^2}{\eta} + \sqrt{100\lambda^2 - 636\frac{\gamma^2\lambda}{\eta} - 855\frac{\gamma^4}{\eta^2}}$ | 1 |
| | | $\frac{1}{6}(-14\lambda - 3\frac{\gamma^2}{\eta} - \sqrt{100\lambda^2 - 636\frac{\gamma^2\lambda}{\eta} - 855\frac{\gamma^4}{\eta^2}}$ | 1 |

than zero, then $14\lambda - 3\frac{\gamma^2}{\eta} > \sqrt{100\lambda^2 - 636\frac{\gamma^2}{\eta}\lambda - 855\frac{\gamma^4}{\eta^2}}$. (Notice that the left-hand side will always be positive since $\lambda < \frac{-3\gamma^2}{2\eta}$.) Squaring both sides of the inequality, combining terms, and factoring out 48 gives us $2\lambda^2 + 15\frac{\gamma^2}{\eta}\lambda + 18\frac{\gamma^4}{\eta^2} > 0$. By factoring, this reduces to $(2\lambda+3\frac{\gamma^2}{\eta})(\lambda+6\frac{\gamma^2}{\eta}) > 0$. In order for this to be satisfied, either $\lambda > \frac{-3\gamma^2}{2\eta}$ or $\lambda < -6\frac{\gamma^2}{\eta}$. These are the opposites of the previous stated inequalities, so there is no region where rectangles will be stable.

In order to consider the zero eigenvalues for rolls and hexagons, we must consider higher order derivatives. From $g(z)$ given in (4.18), we can calculate $dg(z)$ for rolls and hexagons in order to determine the eigenvector associated with the zero eigenvalue. I will write $g$ in real coordinates as was done in (2.8), and will calculate $dg_{(x,y)}$.

For rolls, we have that

$$dg(\sqrt{\frac{-\lambda}{6\eta}},0,0,0,0,0) = \begin{bmatrix} -4\lambda & 0 & 0 & 0 & 0 & 0 \\ 0 & -2\lambda & \gamma\sqrt{\frac{-6\lambda}{\eta}} & 0 & 0 & 0 \\ 0 & \gamma\sqrt{\frac{-6\lambda}{\eta}} & -2\lambda & 0 & 0 & 0 \\ 0 & 0 & 0 & 0 & 0 & 0 \\ 0 & 0 & 0 & 0 & -2\lambda & -\gamma\sqrt{\frac{-6\lambda}{\eta}} \\ 0 & 0 & 0 & 0 & -\gamma\sqrt{\frac{-6\lambda}{\eta}} & -2\lambda \end{bmatrix},$$

so the zero eigenvalue is $(0,0,0,1,0,0)$, so we need to consider higher order derivatives only with respect to $y_1$. Evaluating the derivatives at the solutions for rolls, I get that $\frac{\partial^3\tilde{V}}{\partial y_1^3} = 72\eta y_1 = 0$ and $\frac{\partial^4\tilde{V}}{\partial y_1^4} = 72\eta > 0$. Thus the rolls are stable on the region found above, namely $\lambda < \frac{-3\gamma^2}{2\eta^2}$.

The matrix $dg$ for hexagons is written in real coordinates as

$$dg(\mathbf{z}) = \begin{bmatrix} 2\lambda{+}84\eta x_1^2 & 6\gamma x_1{+}48\eta x_1^2 & 6\gamma x_1{+}48\eta x_1^2 & 0 & 0 & 0 \\ 6\gamma x_1{+}48\eta x_1^2 & 2\lambda{+}84\eta x_1^2 & 6\gamma x_1{+}48\eta x_1^2 & 0 & 0 & 0 \\ 6\gamma x_1{+}48\eta x_1^2 & 6\gamma x_1{+}48\eta x_1^2 & 2\lambda{+}84\eta x_1^2 & 0 & 0 & 0 \\ 0 & 0 & 0 & 2\lambda{+}60\eta x_1^2 & -6\gamma x_1 & -6\gamma x_1 \\ 0 & 0 & 0 & -6\gamma x_1 & 2\lambda{+}60\eta x_1^2 & -6\gamma x_1 \\ 0 & 0 & 0 & -6\gamma x_1 & -6\gamma x_1 & 2\lambda{+}60\eta x_1^2 \end{bmatrix},$$

where $\mathbf{z} = (x_1, x_1, x_1, 0, 0, 0)$ and $x_1 = \frac{1}{60\eta}(-3\gamma \pm \sqrt{9\gamma^2 - 120\eta\lambda})$. For each of these two values of $x_1$, we have that $2\lambda + 60\eta x_1^2 = -6\gamma x_1$. This means that the lower right 3×3 submatrix has the same entries in each position, so the zero eigenvalues correspond to the eigenvectors $(0,0,0,-1,0,1)$ and $(0,0,0,-1,1,0)$. A linear combination of these vectors can be written as $u = a(0,0,0,-1,0,1) + b(0,0,0,-1,1,0)$ where $a$ and $b$ are constants. Then

we can find the partial derivatives of $\tilde{V}$ along any such vector $u$. This can be done as

$$\sum_{i,j,k=1}^{3} u_{i+3}u_{j+3}u_{k+3}\frac{\partial^3\tilde{V}}{\partial y_i \partial y_j \partial y_k}.$$

Notice that any third partial of $\tilde{V}$ with repect to the $y$ variables evaluated at $y = 0$ will be zero. The fourth partial of $\tilde{V}$ along the direction $u$ is given by

$$\sum_{i,j,k,l=1}^{3} u_{i+3}u_{j+3}u_{k+3}u_{l+3}\frac{\partial^4\tilde{V}}{\partial y_i \partial y_j \partial y_k \partial y_l}$$
$$= \eta\{72a^4 + 288a^2(a+b)^2 + 72(a+b)^4 + 288a^2b^2 + 288(a+b)^2b^2 + 72b^4\}.$$

It is easy to see that this is always positive. Thus the hexagons are stable on the region found above, namely if $-\frac{6\gamma^2}{\eta} < \lambda < 0$, then III$^+$ is stable when $\gamma < 0$ and III$^-$ is stable when $\gamma > 0$.

## 4.4 Parlinski's 3-D model

In addition to the two-dimensional model that we considered in the previous chapter, Parlinski and Chapuis also proposed a hexagonal three-dimensional model that they used to study the effects of the molecular dynamics technique [28, 29]. The model is very similar to the two-dimensional model, the only difference being the interaction of particles with those directly above and below it. The hexagonal lattice and its reciprocal space are pictured in Figure 4.3.

The energy function is then written as

$$\begin{aligned} V = \frac{1}{2}\sum_{j,l,n}\{&Ax_{j,l,n}^2 + Bx_{j,l,n}(x_{j+1,l,n} + x_{j-1,l,n} + x_{j,l+1,n} + x_{j,l-1,n} + x_{j+1,l+1,n} + x_{j-1,l-1,n}) \\ &+ x_{j,l,n}(x_{j+1,l-1,n} + x_{j-1,l+1,n} + x_{j+2,l+1,n} + x_{j-2,l-1,n} + x_{j+1,l+2,n} + x_{j-1,l-2,n}) \\ &+ Cx_{j,l,n}(x_{j,l,n+1} + x_{j,l,n-1}) + Hx_{j,l,n}^3 + x_{j,l,n}^4)\} \end{aligned} \tag{4.18}$$

where the indices $j$, $l$, and $n$ are summed over the entire lattice, where the lattice size is $N \times N \times M$ and periodic boundary conditions are assumed.

Because of the only minor changes from the two-dimensional model, this energy function reduces to an energy of the form of 4.14. Specifically, the discrete Fourier transformation

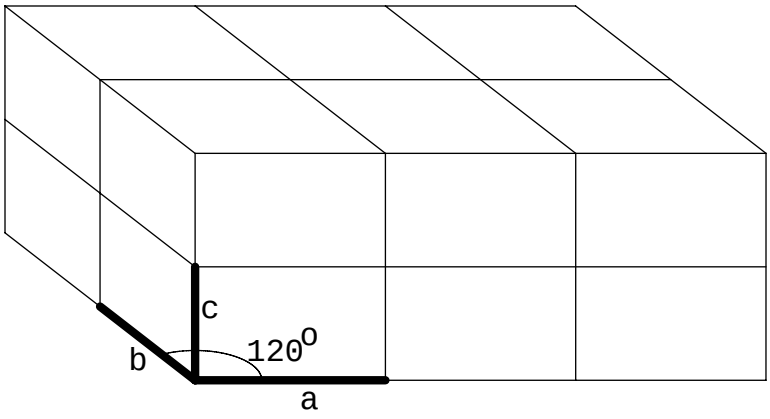


Figure 4.3: The hexagonal lattice for the three-dimensional model.

changes 4.18 to

$$\begin{aligned} V = \frac{N^2}{2}\{ &\sum_{\mathbf{k}_1,\mathbf{k}_2} \lambda(\mathbf{k}_1) z_{\mathbf{k}_1} z_{\mathbf{k}_2} \delta(\mathbf{k}_1 + \mathbf{k}_2 - \tau_1) \\ &+ H \sum_{\mathbf{k}_1,\mathbf{k}_2,\mathbf{k}_3} z_{\mathbf{k}_1} z_{\mathbf{k}_2} z_{\mathbf{k}_3} \delta(\mathbf{k}_1 + \mathbf{k}_2 + \mathbf{k}_3 - \tau_2) \\ &+ \sum_{\mathbf{k}_1,\mathbf{k}_2,\mathbf{k}_3,\mathbf{k}_4} z_{\mathbf{k}_1} z_{\mathbf{k}_2} z_{\mathbf{k}_3} z_{\mathbf{k}_4} \delta(\mathbf{k}_1 + \mathbf{k}_2 + \mathbf{k}_3 + \mathbf{k}_4 - \tau_3)\}. \end{aligned} \tag{4.19}$$

where the coefficient of the quadratic term is given by

$$\begin{aligned} \lambda(\mathbf{k}_1) =& A + 2B[\cos 2\pi n + \cos 2\pi m + \cos 2\pi(n+m)] \\ &+ 2[\cos 2\pi(n-m) + \cos 2\pi(2n+m) + \cos 2\pi(n+2m)] + 2C\cos 2\pi p. \end{aligned} \tag{4.20}$$

Since we are now using three dimensions, the position of an atom is given by the lattice vector $\mathbf{R}_{j,l,n} = j\mathbf{a} + l\mathbf{b} + n\mathbf{c}$ and the reciprocal space vectors are represented as $\mathbf{k}_\alpha = \frac{2\pi n_\alpha}{N}\mathbf{a}^* + \frac{2\pi m_\alpha}{N}\mathbf{b}^* + \frac{2\pi p_\alpha}{N}\mathbf{c}^*$.

Now we can again find approximate solutions by considering the first order approximation of $V$. We will still have all $z$'s be zero except for six. Since $z_{\mathbf{k}} = \bar{z}_{-\mathbf{k}}$, we can refer to only three of the nonzero amplitudes, namely $z_1$, $z_2$, and $z_3$. Then the energy will reduce to

$$\begin{aligned} V =& \frac{1}{2}\{2\lambda(z_1^2 + z_2^2 + z_3^2) + 12Hz_1z_2z_3 + 6(z_1^4 + z_2^4 + z_3^4) \\ &+ 24(z_1^2z_2^2 + z_1^2z_3^2 + z_2^2z_3^2)\} \end{aligned} \tag{4.21}$$

where $\lambda$ is the value of the dispersion function. This is exactly the reduced form of the two-dimensional energy, so we expect the bifurcation diagram to be that in Figure 4.2.

Indeed, Parlinski says that the ground state phase diagram of this model is exactly the same as that of the two-dimensional model (Figure 3.3), except that the parameter $A$ has to be replaced with $A + 2C$.

Therefore, we see that making the model more realistic by including the third dimension still does nothing to allow the model to follow the transition of quartz correctly.

## 4.5 Conclusion

We have now examined models on hexagonal lattices extensively. Specifically, we have done the following:

- We have reviewed work on bifurcation on the hexagonal lattice by Golubitsky and others [14, 22] and have extended their results to cases not considered in those papers.
- We examined a hexagonal model proposed by Parlinski *et al.* [30]. We verified their computations of the ground state phase diagram. We then extended their results by finding other stable and unstable solutions and by drawing the phase diagram showing all of these solutions.
- We proposed and examined modifications to Parlinski's model in the attempt to find a model which exhibited the correct sequence of phase transitions. We used our extensions of Golubitsky's work to show that the phase diagram for all possible modifications is essentially the same as that of Parlinski's original model.

In the future, we propose to do the following:

- Based on the form of (3.4), it is easy to see that 12 reciprocal lattice vectors have equal values of the dispersion function:
$$\begin{aligned}\omega^2(n,m) &= \omega^2(-n,-m) = \omega^2(m,n) = \omega^2(-m,-n)\\ &= \omega^2(n,-n-m) = \omega^2(-n,n+m) = \omega^2(n+m,-n) = \omega^2(-n-m,n)\\ &= \omega^2(m,-n-m) = \omega^2(-m,n+m) = \omega^2(n+m,-m) = \omega^2(-n-m,m).\end{aligned}$$
While we have calculated the minimum of $\omega^2$ along the high-symmetry directions, it is unclear how to minimize the dispersion function for any vector in reciprocal space. If minima occur at a general point in reciprocal space, it is possible that the energy would reduce to a function of 6 displacements rather than 3, as in (3.5).
- James [24] proposed a multilattice for quartz similar to that shown in Figures 1.3 and 1.4. Using methods for multilattices proposed by Pitteri [31], we hope to analyze the bifurcation diagram for a model proposed on James' lattice. Because the model does not use a simple lattice, the discrete Fourier transformation does not work as nicely as it did for Parlinski's model.

# Bibliography


[1] K. Abe, K. Kawasaki, K. Kowada, and T. Shigenari, Effect of uniaxial-stress on central peaks in the 1q and 3q incommensurate phase of quartz, *Journal of the Physical Society of Japan,* **60** (2): 404-407, 1991.

[2] N.W. Ashcroft and N.D. Mermin, *Solid State Physics,* Holt, Rinehart and Winston, New York, 1976.

[3] T.A. Aslanian and A.P. Levanyuk, On the possibility of the incommensurate phase near $\alpha$-$\beta$ transition point in quartz, *Solid State Communications,* **31**: 547-550, 1979.

[4] T.A. Aslanian, A.P. Levanyuk, M. Vallade, and J. Lajzerowicz, Various possibilities for formation of incommensurate superstructure near the $\alpha$-$\beta$ transition in quartz, *Journal of Physics C—Solid State Physics,* **16**: 6705-6712, 1983.

[5] J.P. Bachheimer, An anomaly in the $\beta$ phase near the $\alpha$-$\beta$ transition of quartz, *Journal de Physique Lettres,* **41L**: 559, 1980.

[6] J.P. Bachheimer, The stripe phase of the beta-inc-alpha transformation of quartz under a uniaxial-stress — optical and dilatometric investigation, *Journal de Physique,* **49** (3): 457-462, 1988.

[7] P. Bastie, F. Mogeon, and C.M.E. Zeyen, Direct neutron observation of a single-q incommensurate phase of quartz at zero stress, *Physical Review B—Condensed Matter,* **38** (1): 786-788, 1988.

[8] G.H. Beall, "Industrial Applications of Silica," in *Silica: Physical Behavior, Geochemistry, and Materials Applications,* P.J. Heaney, C.T. Prewitt, and G.V. Gibbs, Editors, Mineralogical Society of America, Reviews in Mineralogy, Vol. 29, 1994.

[9] R. Blinc and A.P. Levanyuk, Editors, *Incommensurate Phases in Dielectrics,* Vol. 2, North Holland, Amsterdam, 1986.

[10] F.D. Bloss, *Crystallography and Crystal Chemistry,* Mineralogical Society of America, Washington, D.C., 1971.

[11] M.B. Boisen and G.V. Gibbs, *Mathematical Crystallography,* Mineralogical Society of America, Washington, D.C., 1990.

[12] P. Borckmans, G. Dewel, and D. Walgraef, Fluctuation effect on the incommensurate transition of quartz, *Journal de Physique I,* **1**: 1055-1062, 1991.

[13] M. Brokate and J. Sprekels, *Hysteresis and Phase Transitions,* Springer-Verlag, New York, 1996.

[14] E. Buzano and M. Golubitsky, Bifurcation on the hexagonal lattice and the planar Bénard problem, *Phylosophical Transactions of the Royal Society of London Series A,* **308**: 617 (1983).

[15] G. Dolino, The $\alpha$-inc-$\beta$ transitions of quartz: A centrury of research on displacive phase transitions, *Phase Transitions,* **21**: 59-72, 1990.

[16] G. Dolino, Incommensurate phase transitions in quartz and berlinite, in *Structural and Magnetic Phase Transitions in Minerals,* S. Ghose, J.M.D. Coey, and E. Salje, Editors, Springer-Verlag, New York, 1988.

[17] G. Dolino and P. Bastie, Phase transitions of quartz, *Key Engineering Materials,* **101-102**: 285-308, (1995).

[18] G. Dolino, P. Bastie, B. Berge, M. Vallade, J. Bethke, L.P. Regnault, C.M.E. Zeyen, Stress-induced 3q-1q incommensurate phase-transition in quartz, *Europhysics Letters,* **3** (5): 601-699, 1987.

[19] M. Golubitsky and D.G. Schaeffer, Imperfect bifurcations in the presence of symmetry, *Communications in Mathematical Physics,* **67**: 205-232, 1979.

[20] M. Golubitsky and D.G. Schaeffer, *Singularities and Groups in Bifurcation Theory,* Vol. I, Springer-Verlag, New York, 1985.

[21] M. Golubitsky, I. Stewart, and D.G. Schaeffer, *Singularities and Groups in Bifurcation Theory,* Vol. II. Springer-Verlag, New York, 1988.

[22] M. Golubitsky, J.W. Swift, and E. Knobloch, Symmetries and pattern selection in Rayleigh-Bénard convection, *Physica D,* **10**: 249-276, 1984.

[23] P.J. Heaney, "Structure and Chemistry of the Low-Pressure Silica Polymorphs," in *Silica: Physical Behavior, Geochemistry, and Materials Applications,* P.J. Heaney, C.T. Prewitt, and G.V. Gibbs, Editors, Mineralogical Society of America, Reviews in Mineralogy, Vol. 29, 1994.

[24] R.D. James, "The stability and metastability of quartz," in *Metastability and Incompletely Posed Problems,* S. Antman, J.L. Ericksen, D. Kinderlehrer, and I. Müller, Editors, IMA Series, Vol. 3, Springer-Verlag, 1987.

[25] H. Le Chatelier, *Sur la dilatation du quartz, Comptes Rendus,* **108**: 1046, 1889.

[26] Y.V. Malov and V.E. Sonyushkin, Direct electron-microscopic investigation of the $\alpha \rightarrow \beta$ transition process in quartz, *Soviet Physics, Crystallography,* **20**: 644-645, 1975.

[27] K. Parlinski, Molecular-dynamics simulation of incommensurate phases, *Computer Physics Reports,* **8**: 153 ,1988.

[28] K. Parlinski and G. Chapuis, Mechanisms of phase transitions in a hexagonal model with 1q and 3q incommensurate phases, *Physical Review, B—Condensed Matter,* **47** (1): 13983-13991, 1993.

[29] K. Parlinski and G. Chapuis, Phase-transition mechanisms between hexagonal commensurate and incommensurate structures, *Physical Review, B—Condensed Matter,* **49** (17): 11643 ,1994.

[30] K. Parlinski, S. Kwiecinksi, and A. Urbanski, Phase diagram of a hexagonal model with incommensurate phases, *Physical Review, B—Condensed Matter,* **46** (9): 5110-5115, 1992.

[31] M. Pitteri, On $(\nu + 1)$-lattices, *Journal of Elasticity,* **15**: 3, 1985.

[32] P. Saint-Grégoire, E. Snoek, V. Janovec, and C. Roucau, New details of the structure of 3-q modulated phase of quartz type, *Physica Status Solidi A,* **139**: 361-370, 1993.

[33] E.K.H. Salje, Application of Landau theory for the analysis of phase transitions in minerals, *Physics Reports,* **215** (2): 49-99, 1992.

[34] D.H. Sattinger, Group representation theory, bifurcation theory, and pattern formation, *Journal of Functional Analysis,* **28**: 58-101, 1978.

[35] A.U. Sheleg and V.V. Zaretskii, List of incommensurate crystals, in *Incommensurate Phases in Dielectrics,* Vol. 2, R. Blinc and A.P. Levanyuk, Editors, North Holland, Amsterdam, 1986.

[36] E. Snoeck and C. Roucau, Electron-microscopy study of the 3q to 1q phase-transition in the incommensurate phase of quartz under stress, *Physical Review B—Condensed Matter,* **45** (22): 12720-12724, 1992.

[37] R.B. Sosman, *The Phases of Silica,* Rutgers University Press, New Brunswick, New Jersey, 1965.

[38] V. Soula, K. Abe, P. Bastie, G. Dolino, B. Capelle, and Y.L. Zheng, Synchrotron and light-scattering observation of the 1q incommensurate phase of quartz under zero-stress, *Physical Review B—Condensed Matter,* **48** (10): 6871-6879, 1993.

[39] F.S. Tautz and V. Heine and M.T. Dove, and X. Chen, Rigid unit modes in the molecular dynamics simulation of quartz and the incommensurate phase transition, *Physics and Chemistry of Minerals,* **18**: 326-336, 1991.

[40] M. Vallade, B. Berge, and G. Dolino, Origin of the incommensurate phase in quartz: II. Interpretation of inelastic neutron scattering data, *Journal de Physique I,* **2** (7): 1481-1495, 1992.

[41] G. Van Tendeloo, J. Van Landuyt, and S. Amelinckx, The $\alpha$-$\beta$ phase transition in quartz and $AlPO_4$ as studied by electron microscopy and diffraction, *Physica Status Solidi A,* **33**: 723-735, 1976.

[42] A. Zarka, B. Capelle, M. Petit, G. Dolino, P. Bastie, and B. Berge, Evidence of a 1q incommensurate phase in quartz by synchrotron x-ray diffraction, *Journal of Applied Crystallography,* **21**: 72-73, 1988.

# Vita

George West Moss III was born in Opelika, Alabama and grew up in Arab, Alabama and Brownsville, Tennessee. After graduating from Haywood High School in 1990, he attended Auburn University where he graduated in 1994 with a Bachelor of Science degree in Applied Mathematics. He then moved to Blacksburg, Virginia (yet another small town in the South) and began graduate school at Virginia Tech. He began working under the advisement of Dr. Robert C. Rogers during the summer of 1996. George enjoyed his work as a teaching assistant and decided to pursue a career in college teaching upon completion of the Doctorate of Philosophy in Mathematics, for which this paper represents the final requirement.